Peripheral and cerebral metabolic features in an animal model of Huntington's disease expressing full-length mutant huntingtin

Carla Maria Nunes Lopes

Coimbra, 2010

Department of Physics
Faculty of Sciences and Technology
University of Coimbra

Dissertação apresentada à Universidade de Coimbra para cumprimento dos requisitos necessários à obtenção do grau de Mestre em Engenharia Biomédica, realizada sob a orientação científica do Professora Doutora Ana Cristina Rego (Universidade de Coimbra)

To my parents

Acknowledgments

This dissertation would not have been possible without the support and help from many people in many different ways. Those people to whom I owe a great deal of thanks I would like to address my appreciation:

First and the foremost, I would like to express my gratitude to my supervisor Professora Doutora Ana Cristina Rego for all the supporting, encouragement and willingness during this last months that make me look to science from a different perspective.

Thanks to Doctor Ana Isabel Duarte, my co-advisor, for all dedication, commitment and enthusiasm that were always present as well as words of encouragement when sometimes thinks were not as perfect as I would expect.

My colleges at Center for Neuroscience and Cell Biology for their support, friendship and good moments spent in laboratory.

My friends for always had been there for me, even in most stressful moments. I specially would like to thanks the true friendship from Vinita, Sofia, André and Luis that made this project much easier.

My family for all their loving and support in all my decisions, giving me strength and courage to keep going.

To all, that directly or indirectly, contribute to the success of this project my true thanks

Table of Contents

Resumo

A doença de Huntington é uma doença autossómica dominante causada pela expansão de uma repetição do trinucleótido CAG no gene *IT15* ou *HD* que codifica a proteína huntingtina (Htt). A repetição de CAG codifica um longo domínio de poliglutaminas nesta proteína, que se acredita conferir um ganho de função deletério. A característica mais importante da doença é a perda neuronal selectiva, principalmente dos *medium spiny neurons* do estriado, e no córtex cerebral, em fases mais avançadas da doença. A neurodegenerescência conduz a um défice motor, sendo os sinais clássicos da doença a coreia e distonia, descoordenação, e problemas comportamentais que conduzem à deterioração cognitiva progressiva. As disfunções metabólicas são relativamente comuns nesta doença, tais como a alteração no metabolismo da glucose, diabetes e alterações na sensibilidade/resistência à insulina. Vários estudos demonstraram que doentes com HD e murganhos transgénicos R6/2 (que expressam o exão 1 da huntingtina mutante, mHtt) possuem uma maior incidência de diabetes. No entanto, nada se sabe sobre o efeito da expressão da mHtt na disfunção metabólica periférica. Os murganhos YAC128 expressam mHtt completa com 128 glutaminas e manifestam um fenotipo próximo dos doentes com HD, incluindo alterações motoras precoces, declínio cognitivo e atrofia e degenerescência estriatal dependente da idade. Estes murganhos foram criados num *background* FVB, sendo mais susceptíveis à desregulação metabólica e resistência à insulina. Assim, o objectivo deste estudo foi avaliar o efeito da hiperglicémia em parâmetros metabólicos periféricos e centrais em murganhos YAC128 *versus wild-type* (WT), com a mesma idade. Os nossos resultados mostraram que os murganhos WT e YAC128 com 6 meses de idade são hiperglicémicos, apresentando glicemia de jejum acima de 130 mg glucose /dl sangue. A diabetes foi avaliada pelos testes de tolerância à glucose e insulina (GTT e ITT, respectivamente). Os murganhos YAC128 não apresentavam alterações significativas no peso corporal, nos níveis plasmáticos de glucose ou no GTT em comparação com os murganhos WT. Porém, no ITT os murganhos YAC128 mostraram uma tendência para uma ligeira redução dos níveis de glucose no sangue após 30 minutos, o que poderá indicar alguma sensibilidade à insulina. No teste comportamental de *rotarod* os murganhos YAC128 demonstraram uma tendência para uma diminuição da latência para cair, sugerindo alguma deficiência motora em murganhos transgénicos, em comparação com os WT. Os níveis plasmáticos de IGF-1 e insulina apresentaram uma tendência para uma redução nos murganhos transgénicos relativamente aos murganhos WT. No cérebro, os níveis de IGF-1 apresentaram uma ligeira tendência para uma diminuição nos animais YAC128, concomitante com uma redução na carga energética e um aumento da razão lactato/piruvato, sugerindo alterações

bioenergéticas neste modelo animais da HD. Os nossos dados sugerem fortemente que a expressão de mHtt em murganhos hiperglicémicos induz alterações metabólicas periféricas e centrais associadas com os níveis de insulina plasmática e com um metabolismo energético cerebral comprometido, que se correlaciona com um défice motor. Este estudo pode ser importante para definir o papel da mHtt na susceptibilidade dos doentes de Huntington para a desregulação metabólica e a ocorrência de diabetes.

Summary

Huntington's disease (HD) is an autosomal dominant disease caused by an expansion of CAG repeats in the gene (*IT15* or *HD* gene) encoding for huntingtin (Htt). The expanded repeat encodes a polyglutamine stretch that is believed to confer a deleterious gain-of-function to the protein. The most significant hallmark of HD is the selective neuronal loss, primarily in the striatum and in cerebral cortex in later stages. This neurodegeneration leads to progressive motor and cognitive deterioration, including chorea and dystonia, incoordination, psychiatric disturbances, cognitive decline and dementia. Metabolic dysfunction is relatively common in this disease and may be caused by impaired carbohydrate metabolism, diabetes and changes in insulin sensitivity. Several studies demonstrated that HD patients and the R6/2 HD transgenic mouse model (expressing the exon-1 of human Htt) show increased incidence of diabetes mellitus. However, nothing is known about the effect of expression of full-length mutant Htt (mHtt) on peripheral metabolic dysfunction. The YAC128 mice express full-length mHtt with 128 glutamines and manifest a phenotype close to HD patients, including early motor abnormalities, cognitive decline and age-dependent striatal atrophy and degeneration. These mice were created in a FVB background, known to be more susceptible to metabolic dysregulation and insulin resistance. Thus, the objective of our study was to evaluate the effect of an hyperglycemic background on peripheral and central metabolic parameters in YAC128 mice *versus* age-matched wild-type (WT) littermates. Our results showed that 6 month-old YAC128 and WT mice were hyperglycemic, exhibiting fasting plasma glucose levels over 130 mg/dl. Diabetes was evaluated by the glucose and insulin tolerance tests (GTT and ITT, respectively). YAC128 mice did not exhibit significant changes in body weight, plasma glucose levels or GTT compared to WT mice. However, in ITT YAC128 mice showed a tendency for a slight reduction in blood glucose levels at 30 minutes, which may indicate some sensitivity to insulin. The rotarod behaviour test showed that YAC128 mice had a tendency for decreased latency to fall off, suggesting some motor impairment in hyperglycemic HD mice, compared to WT littermates. In transgenic mice, plasma levels of IGF-1 and insulin were slightly, although not significantly, decreased. In brain, IGF-1 levels showed a slight tendency for a reduction in YAC128 mice, concomitantly with a reduction in energy charge and higher lactate/pyruvate ratio, probably as a result of bioenergetic abnormalities in HD mice. Our data highly suggest that expression of full-length mHtt in hyperglycemic background induces both peripheral and central metabolic changes, which may result from altered plasma insulin levels, and deficient brain energy metabolism associated with motor impairment. This

study may be important for defining the role of mHtt in the susceptibility of HD patients to undergo metabolic deregulation and diabetic features.

PART I

GENERAL INTRODUCTION AND METHODS

CHAPTER I

GENERAL INTRODUCTION

1.1. Huntington's disease

Huntington's disease (HD) is a fatal neurodegenerative disorder that was first described by George Huntington in 1872. He published his report on a hereditary form of chorea in *The Medical and Surgical Reporter* (Huntington, 1872).

In his writing, he describes the disease in an accurate way, referring *"three marked peculiarities in this disease:*

1. Its hereditary nature.

2. A tendency to insanity and suicide.

3. Its manifesting itself as a grave disease only in adult life"

Despite Mendel's Laws describing the principle of hereditary transmission were still recent and weakly disseminated, Huntington was able to note the autosomal dominant inheritance:

> *"The hereditary chorea, as I shall call it, is confined to certain and fortunately a few families, and has been transmitted to them, an heirloom from generations away back in the dim past……. When either or both the parents have shown manifestations of the disease, and more especially when these manifestations have been of a serious nature, one or more of the offspring almost invariably suffer from the disease, if they live to adult age. But if by any chance these children go through life without it, the thread is broken and the grandchildren and great-grandchildren of the original shakers may rest assured that they are free from the disease."*

The average onset is about 40 years, ranging from 1 to 80 years (Nance *et al.*, 2001;for review, Walker, 2007), progressing inexorably to death 15-20 years after the onset (for review, Rego *et al.*, 2005). Only about 5-7% of patients exhibit symptoms before 21 years-old, in what was defined as the juvenile form of HD (Nance *et al.*, 2001).

In early stages of the disease there are subtle psychiatric changes that are often misunderstood, since they are not severe enough to be recognized on their own. HD is associated with movement disorder (also named *chorea*) which becomes worse over the course of disease, but also involves emotional and cognitive disturbances, leading to dementia, as described in section 1.1.3.

1.1.1. Epidemiology

HD is one of the most important genetic disorders of adulthood.

Europe has the largest number of prevalence studies and, as it can be seen in Figure 1.1., an uniform prevalence of HD. Indeed, a prevalence of 4-7 per 100,000 people is found over a large part of the continent. Finland reveals an atypical low prevalence, of about 0.5 per 100,000 individuals, which can be related to genetically distinct features from other populations, probably diverged from the common origin before such mutations occurred (Harper, 1992). A previous study in South Wales found a prevalence of 8.85 HD cases per 100,000 people (Quarrell, 1988).

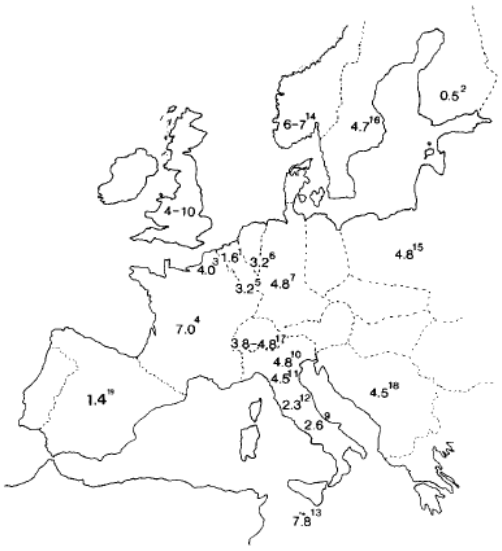

Fig. 1.1. HD prevalence in various European countries. There is a high prevalence rate for HD in most European countries where it has been intensively studied; Finland is an exception [Harper, 1992].

Table I. Prevalence estimates for HD in Europe (excluding UK)

Country	Map no.	Author	Prevalence per 100,000
Belgium	1	Husquinet (1970)	1.63
Finland	2	Palo et al. (1987)	0.5
France			
(Northern)	3	Petit (1970)	4.0
(Haute Vienne)	4	Leger et al. (1974)	4.8
Germany			
(Rhineland)	5	Panse (1942)	3.2
(Kassel)	6	Wendt and Drohm (1972)	3.2
(Federal Republic)	–	Wendt and Drohm (1972)	2.2
(Franconia)	7	Przuntek and Steigerwald (1987)	4.8
Iceland	8	Gudmundsson (1969)	2.7
Italy			
(Lazio)	9	Frontali et al. (1990)	2.56
(Emilia)	10	Mainini et al. (1982)	4.8
(Liguria)	11	Roccatagliata and Albano (1976)	4.5
(Toscana)	12	Arena et al. (1979)	2.34
(Florence)		Groppi et al. (1986)	4.1
Malta	13	Cassar (1967)	7.8
Norway	14	Saugstad and Odegard (1986)	6.7
Poland	15	Cendrowski (1964)	4.8
Spain	19	Ordonez (1970)	1.4
Sweden	16	Mattsson (1974)	4.7
Switzerland	17	Zölliker (1949)	3.8–4.8
Yugoslavia			
(Rijeka district)	18	Sepcic et al. (1989)	4.46

Based on Harper (1992)

HD was originally described in North America, in families of British descent, as confirmed by the elevated rate of occurrence in descendents of Western European. In 2000, there were 30,000 cases of HD in United States, indicating a prevalence of about 10 cases per 100,000 people. The prevalence of HD in African Americans generates some controversy. Some studies described a much lower rate (Wright *et al*., 1981), but this number was refuted by the Maryland study, which found a prevalence of 5.15 per 100,000 people, based on a population of 4,217,000, a similar number to the population of Western-European origin. In most of these affected families, the HD allele did not have an European origin (Folstein *et al.,* 1987).

In Portugal. the prevalence of HD is estimated to range from 2-5 per 100,000 people, overlapping the european values (Costa *et al.,* 2003).

The disorder is rare in Orientals and Africans, suggesting that HD gene is rare (Harper, 1992). Japan has a very low rate, of about 0.5 per 100,000 people (Walker, 2007). In contrast, there are some regions where the prevalence is unusually high. Some studies were able to track the ancestor by genealogical analysis, mainly due to historical migration and geographic isolation of these areas. Tasmania has a prevalence of 17,4/100,000 people and the region of Lake Maracaibo, Venezuela, has more than 100 living HD patients, all descended from a single ancestor (Conneally, 1984; Harper, 1992). Importantly, HD affects equally males and females. The total heterozygote frequency in South Wales has been estimated at 20.2 per 100,000 people (Conneally, 1984).

1.1.2. Genetics

An expansion of cytosine-adenine-guanine (CAG) repeats was first described in the androgen gene, and since then a class of nine genetically distinct, gain-of-function disorders were described, constituting the polyglutamine-expansion diseases. These include HD, dentatorubralpallidoluysian atrophy, spinal bulbar muscular atrophy (SBMA) or Kennedy's disease and spinocerebellar ataxias 1, 2, 3, 6, 7 and 17 (Table II) (Bates, 2005).

The gene affected in HD encodes the protein huntingtin (Htt) and the mutation results in a stretch of glutamine residues located at the N-terminal of mutant Htt (mHtt) (The Huntington's Disease Collaborative Research Group, 1993). This is believed to confer a deleterious gain-of-function to the mutant protein. The HD gene was mapped in 1983 with the eight polymorphic marker test (G8), which mapped the gene to chromosome 4 (4p) (Gusella *et al.,* 1983). However, the HD gene was cloned only in 1993, which allowed the identification of a coding region occurring at the short arm of chromosome 4 *(*4p16.3), corresponding to an unstable DNA segment containing an

expansion of a polymorphic trinucleotide repeat, near the 5' end in the exon 1 of the *"Interesting Transcript 15"* (IT15) gene, that spans over 200 kb and is composed of 67 exons (The Huntington's Disease Collaborative Research Group, 1993).

Table II Polyglutamine Expansion Diseases

Polyglutamine disorder CAG	Protein product/ Locus	Normal and Pathogenic repeat number	Primary target of neuropathology
Dentatorubro-pallidoluysian atrophy (DRPLA)	Atrophin 1 12p12	3-35 49-88	Cerebellum (dentate nucleus), red nucleus, globus pallidus (external segment), subthalamic nucleus
Huntington's disease (HD)	Huntingtin 4p16.3	6-35 36-121	Caudate nucleus (medium spiny neurons), putamen, globus pallidus (external segment)
Spinal and bulbar muscular atrophy (SBMA;Kennedy disease)	Androgen receptor Xq11-q12	9-36 38-62	Motor neuron in anterior horn cells of the spinal cord and brainstem
Spinocerebellar ataxia 1 (SCA1)	Ataxin 1 6p23	6-38 39-83	Cerebellum, red nucleus, inferior olive, pons,anterior horn cells and pyramidal tracts
Spinocerebellar ataxia 2 (SCA2)	Ataxin 2 12q24	14-31 32-77	Cerebellar Purkinje cells, cytoplasmatic inclusions
Spinocerebellar ataxia 3 (SCA3)	Ataxin 3 14q24.3-q31	12-40 54-86	Cerebellar dentate neurons, basal ganglia, brain stem, spinal cord
Spinocerebellar ataxia 6 (SCA6)	Ca2+channel 19p13	4-19 20-30	Cerebellar Purkinje cells, dentate nucleus, inferior olive, cytoplasmatic inclusions
Spinocerebellar ataxia 7 (SCA7)	Ataxin 7 3p21.1-p12	4-35 37-200	Cerebellum, brain stem, macula, visual cortex
Spinocerebellar ataxia 17 (SCA17)	TATA-binding protein (TBP) 6q27	29-42 47-55	Cerebellum, cortex (diffuse atrophy), caudate and putamen. NII

Based on Rego and de Almeida, 2005.

Normal alleles are defined as alleles with $\leq$ 26 CAG repeats; these are non-pathologic and segregated as a stable polymorphic repeat in > 99% of meiosis. In normal individuals, the most frequent allele length contains 17 and 19 CAG repeats (Kremer *et al*., 1994)

Mutable normal alleles are defined as alleles with 27-35 CAG repeats. This repeat range is often referred to as the meiotic instability range or as "intermediate alleles". No case has been associated unequivocally with an HD phenotype (Rubinsztein *et al*., 1996, Brinkman *et al*., 1997), but they can be meiotically unstable in sperm, and predispose to CAGs expansion from one generation to the next, particularly when the disease is transmitted by males (Myers *et al*. 1993; Rubinsztein *et al*., 1996). This susceptibility was only described during transmission through the male germline and is associated with advanced paternal age (Goldberg *et al*., 1993).

HD alleles with reduced penetrance are defined as having 36-39 CAG repeats; these are meiotically unstable and associated with HD phenotype in both clinically and neuropathologically documented cases (Nance *et al.*, 2001). Few asymptomatic individuals over 75 years, with this allele size, have been documented (Rubinsztein *et al*., 1996).

Alleles with ≥ 40 CAG repeats are defined as alleles with full penetrance. While there are several reports of elderly clinically asymptomatic HD gene carriers with 40 and 41 CAG repeats, no individuals with >41 CAG repeat length remained asymptomatic after middle life and the probability of an earlier onset is inversely related to number of CAG repeats (Brinkman *et al*., 1997). The presence of ≥ 60 CAGs is associated with juvenile onset that represents approximately 5-7% of all cases (Nance, 2001). A few cases of juvenile-onset disease with more than 200 CAG repeats have been documented (Nance *et al*., 1999; Seneca *et al.*, 2004) (Figure 1.2.)

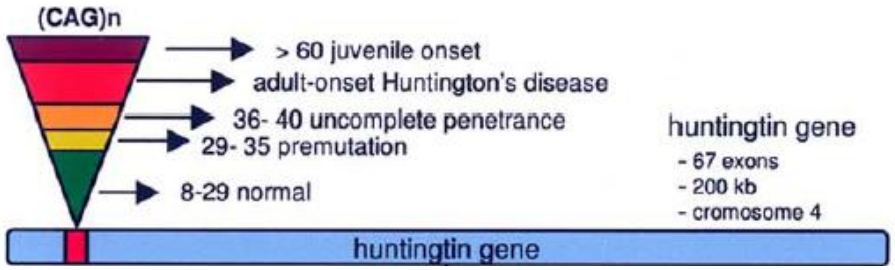

Fig. 1.2. Representation of the HD gene and the impact of polyglutamine repeat size on HD onset [Adapted from Rego and de Almeida, 2005]

As an autosomic dominant disorder, the HD offspring have 50% chance of inheriting the disease in a Mendelian mode.

The number of polyglutamines is inversely correlated with age of onset (Duyao, 1993, Nørremølle, 1993), but this only accounts for about 40% of the variation, with the remaining due to genetic polymorphisms adjacent to CAG repeat (for review, Rego and Almeida, 2005) and environment (Wexler, 2004). However, some studies did not find a relationship between the number of CAG repeats and the rate of clinical decline (Kieburtz, 1994), which suggested that CAG repeat length may have a small effect on the rate of progression that may be clinically important over time (Rosenblatt, 2006).

A large population sample was analyzed in Portugal, showing that CAG ranged between 9 and 40 repeats, with the 17 CAG allele occurring most frequently (37.9%). Intermediate alleles with

27–35 CAGs represented 3.0% and two expanded alleles (0.11%) were found, one of reduced penetrance (36 CAGs) and other with fully penetrant repeat (40 CAGs) (Costa *et al.,* 2006).

The number of CAG repeats is only highly predictive of the age of onset if CAG≥ 40. The genes encoding for NR2A/B receptor subunits of the *N*-methyl-D-aspartate (NMDAR) receptor may be responsible for the variance on the age of onset in individuals with CAG repeat lengths between 30-40 (Arning *et al.,* 2005). In a cohort of HD patients with a CAG repeat length between 41 and 45, 30.8% of the variance in age of onset could be attributed to CAG repeat number, while variations in the NR2A (*N*-methyl-D-aspartate receptor receptor subunit) and NR2B genes accounted for 4.5% and 12.3% of the variance, respectively (Arning *et al.,* 2005)

1.1.3. Clinical aspects

HD symptoms typically manifest in midlife, between 35-50 years old and become fatal 15-20 years after the onset and juvenile or late-onset forms have shorter disease (Foroud *et al.,* 1999) (Figure 1.3.).

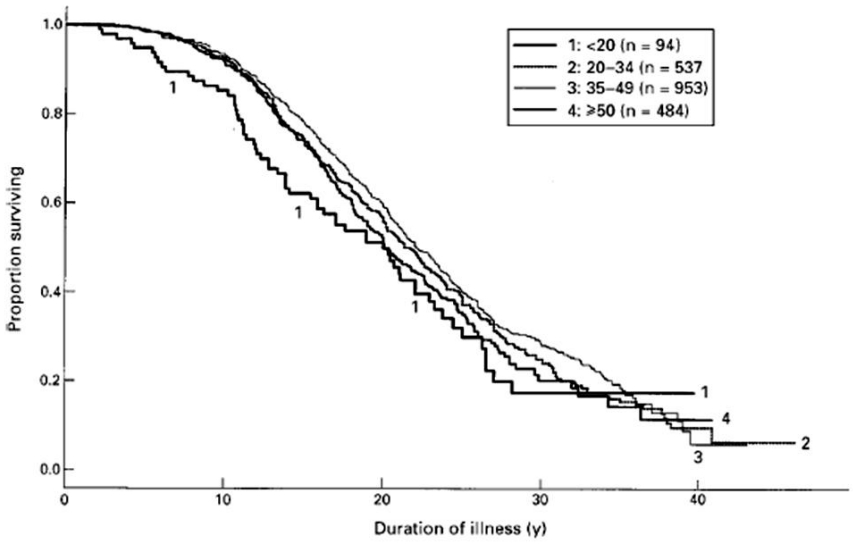

Fig. 1.3. Survival curves. The mean illness duration is higher for the second group (20-34 years old) and significantly shorter among juvenile (< 20 years old) and late onset patients (> 50 years old, having this two groups a similar duration (Foroud *et al.,* 1999).

Psychiatric and behavioral problems usually appear early in the course of the disease and are major constituents of the clinical spectrum of HD (Duijn *et al*., 2007).The disease it's classically

associated with progressive emotional, cognitive, and motor disturbances. In a presymptomatic phase (prodromal phase), relatively subtle symptoms (*e.g.* changes in personality, cognition, and motor control) may precede the disease onset by several years. Irritability or disinhibition, difficulty in developing multitasking, forgetfulness and anxiety are common, depression, impulsiveness, apathy and also motor changes including minor difficulties in coordination, balance, and slight adventitious movements of the trunk, limbs, and finger can be present (for review, Walker, 2007; Foroud *et al.*, 1999). Oculomotor abnormalities are primordial features and often the earliest motor sign; delayed initiation and slowing of saccadic movements, and inability to suppress glances at novel stimuli and an occasional nystagmus (Leigh *et al.*, 1983).

One of the most characteristic sign of HD is both involuntary and voluntary movement disorders. Involuntary movements were first described by George Huntington as *Chorea*, derived from the Greek word *χορεία* (a kind of dance). Choreoathetotic movements are clonic spasm affecting voluntary muscles, with a random pattern. The severity varies from restlessness with mild, intermittent exaggeration of gesture and expression, through fidgety movements of hands and unstable dance-like gait, to a continuous flow of disabling and violent movements (Wild *et al.*, 2007). Motor symptoms commonly begin by slight twitchings in the muscles of the face, which gradually increase in violence and variety, which may interfere with vocalization, chewing and swallowing. Dysarthria and dysphagia are common in these patients (for review, Walker, 2007).

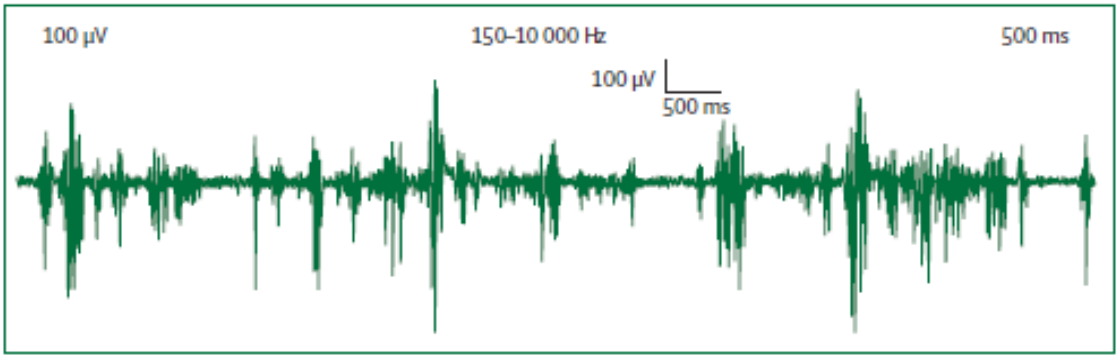

Fig. 1.4. EMG recording of chorea in a patient in stage I HD.
Recording is made with standard belly tendon, using surface disc electrodes placed over the first dorsal interosseus muscle. Graph presents an irregular pattern of discharges, with variable amplitude, duration, and rise times of every EMG burst. Healthy individuals at rest show no EMG activity (Walker, 2007).

Voluntary movements are also disturbed, leading to bradykinesia and rigidity with slow initiation and poor execution of coordinated movements, especially in later stages of the disease (Purdon *et al.*, 1994). In children with the juvenile form, a dominant picture of bradykinesia, rigidity, dystonia, ataxia and epileptic seizures occurs (Seneca *et al.*, 2004; Ruocco *et al.*, 2006). Another finding in HD that contributes to patients' overactivity is motor 'impersistence' — the inability to maintain a voluntary muscle contraction at a constant level. In Figure 1.4. an electromyography (EMG) (recording of electrical activity of skeletal muscle) recording of chorea in patient with stage I HD shows a variable and random patterns of muscle activation with short duration bursts common in HD. Incapacity to apply steady pressure during handshake is characteristic of HD and is called *milkmaid's grip*. Motor 'impersistence' is a good marker of disease severity, since it is independent of chorea and linearly progressive. Fine motor skills, such as finger-tapping rhythm and rate, are useful for establishing an early diagnosis of HD (Walker, 2007). Although chorea is the cardinal feature of HD, a significant percentage of patients do not refer it as the first symptom; rather, the patients refer other prominent symptoms, like cognitive or emotional changes (Foroud *et al.*, 1999).

Table III – First symptoms *of HD*

Symptom	*No of patients* **	*% all observed symptoms* †
Chorea	877	28
Trouble walking	262	9
Unsteadiness/imbalance	260	8
Difficult to get along with	167	5
Depression	165	5
Clumsiness	154	5
Speech difficulty	149	5
Memory loss	93	3
Trouble holding an object	62	2
Lack of motivation	53	2
Suspicions/paranoia	48	2
Intellectual decline	44	1
Changes in sleep	30	1
Hallucinations	23	1
Weight loss	20	0.6
Sexual problems	7	0.2
Sadness	7	0.2
Other mental	363	12
Other physical	297	10

Number of patients is reported from a total of 1901 patients with initial symptom information. Percentage of all observed symptoms from a total of 3086 reported symptoms. Patients could report up to three initial symptoms (Foroud *et al.*, 1999).

Several studies showed a high frequency of psychiatric disturbances in HD (Table III). Depressive symptoms could be a direct result of brain degeneration or a psychological reaction to the disease. Affective component is a major concern given the high risk of suicide, estimated to be 5-10 times more frequent than in general population (Duijn *et al.*, 2007; for review Walker, 2007).

As disease progresses, memory deficits tend to appear. Reported impairments range from short-term memory deficits to long-term memory difficulties, including deficits in procedural and working memory. Cognitive problems tend to get worse over time and, in late-stage HD, leads to dementia (Montoya *et al.,* 2006).

Sleep disturbances are also common clinical problems in HD and include increased sleep onset latency, reduced sleep efficiency, disruption of sleep, more time spent awake and less slow wave sleep. These abnormalities appear to be related with duration and severity of the disease, and degree of atrophy of the caudate nucleus. Patients also show an increased density of sleep spindles (Wiegand *et al*., 1991, Hansotia *et al.,* 1995, Cuturic *et al*., 2009). Recently, it was shown that HD patients have a disrupted circadian rhythm (Morton *et al*., 2005) probably due to melatonin deficiency (Alders *et al.,* 2009).

Interestingly, the most frequent primary cause of death in HD is pneumonia and cardiovascular disease (Sørensen *et al.,* 1992).

1.1.4. Neuropathology

Basal ganglia are a group of nuclei located subcortically that are involved in motor and cognitive processes. Cerebral cortex and *substantia nigra pars compacta* (SNpc) send glutamatergic and dopaminergic inputs, respectively, to caudate and putamen, and frontal cortex receives transiently excitatory input from the thalamus (Purves *et al.,* 2004). Connections between basal ganglia output nuclei (GPi/SNr) (globus pallidus interna/ substancia nigra *pars reticulata*) and striatum are organized in two pathways: direct and indirect.

The direct pathway is a "monosynaptic" transiently inhibitory projection between medium spiny neurons (MSN) of caudate and putamen to the tonically active inhibitory neurons in GPi/SNr, which in turn provides inhibitory innervation to thalamocortical projections (ventral anterior and ventral lateral thalamic nuclei - VA/VL complex).

The indirect pathway is a "polysynaptic" connection that involves intercalated neurons in globus pallidus externa *(*GPe) and STN (subthalamic nucleus) and increases the level of tonic

inhibition. Ninety-five per cent of all neurons in striatum are GABAergic and contain mainly the inhibitory neurotransmitter γ-aminobutyric acid (GABA) and enkephalin, dynorphin or substance P (SP) as co-transmitter. When the indirect pathway is activated by excitatory signals from the cortex, MSN discharge and inhibit tonically active GABAergic neurons of GPe. These neurons project to STN, which in turn sends excitatory inputs to GPi and SNpr that oppose the disinhibitory action of the direct pathway. Thus, indirect pathway modulates the direct pathway. Most MSNs express D1 (subtype 1 dopamine receptor) and D2 (subtype 2 dopamine receptor) receptors, the majority of D1-expressing neurons being part of direct pathway and containing substance P, whereas D2- bearing neurons are part of indirect pathway, projecting to GPe and contain enkephalin (Purves *et al.,* 2004).

SNr also projects its axons to deep layers of superior colliculus, an area of the upper motor neurons that command the *saccades* (rapid orienting movements of the eyes). Immediately before saccade onset, discharge rate of reticulata neurons is greatly reduced through the input from tonic GABAergic MSNs of caudate, which have been activated by signals from cortex. As a consequence upper motor neurons of superior colliculus is activated, allowing them to generate bursts of action potentials that command the saccade (Purves *et al.,* 2004).

In patients with HD, MSN that project to the external segment of GP degenerate, especially those synthesizing enkephalin and GABA. In absence of their normal inhibitory input from spiny neurons, GPe cells become abnormally active; in turn, this activity reduces the excitatory output of STN to GPi, leading to the reduction of the inhibitory outflow of the basal ganglia (Figure 1.5.), (Purves *et al.,* 2004).

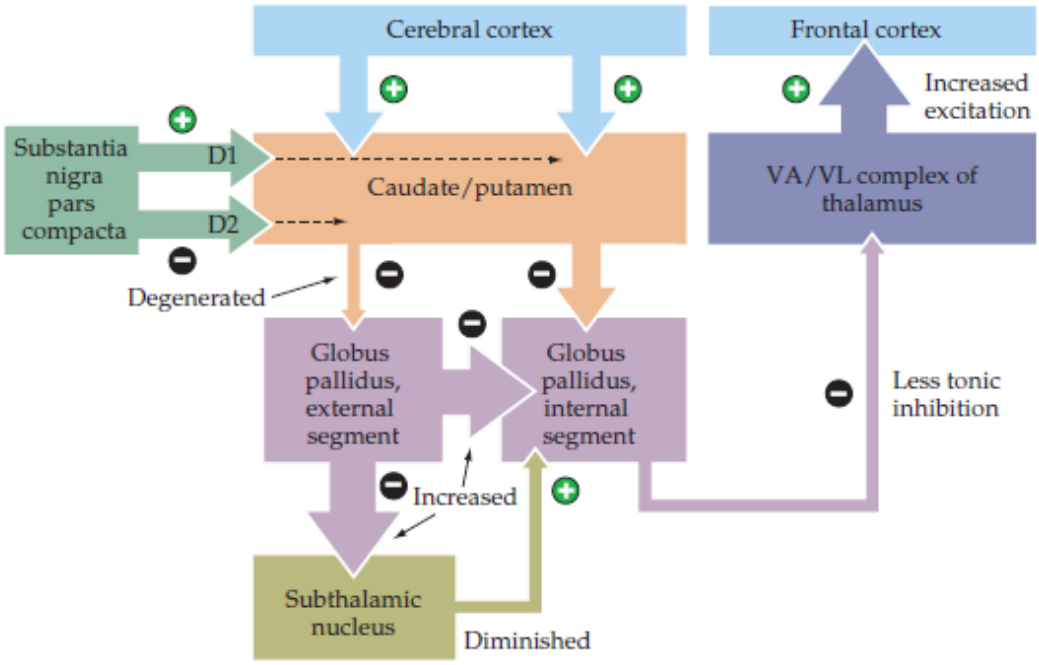

Fig.1.5. Direct and indirect pathways through basal ganglia in HD. The balance of inhibitory signals in direct and indirect pathways is altered, leading to a decrease ability of basal ganglia to control the thalamic output to cortex. Projection from caudate and putamen to GPe is decrease (thinner arrow). This effect increases the tonic inhibition from GP to STN (larger arrow), making the excitatory STN less effective in opposing the action of direct pathway (thinner arrow). Thus, thalamic excitation of cortex is increased (larger arrow), leading to greater and often inappropriate motor activity. VA -ventral anterior thalamic nuclei; VL-ventral lateral thalamic nuclei (Purves *et al*., 2004).

Without the restricting influence of basal ganglia, upper motor neurons can be activated by inappropriate signals, resulting in choreatic movements and slowing of saccadic movements(Purves *et al.*, 2004).

As mentioned before, basal ganglia are also involved in other *non-motor* functions with significant clinical implications. Degeneration of specific subdivisions of prefrontal and limbic loop appears to be related with deterioration of cognitive and emotional function typical in HD (Purves *et al.*, 2004). The prefrontal loop regulates the initiation and termination of cognitive processes (*e.g.* planning, working memory and attention) and the limbic loop regulates emotional behavior and motivation (Purves *et al.*, 2004).

Degeneration can be found at different degrees in MSNs. In early and middle stage HD, enkephalinergic striato-GPe projection and SP-containing projection to SNr (indirect pathway) are more severely affected than SP -containing projections to the GPi and SN (direct pathway), resulting in an imbalance between the direct and indirect pathways. A possible explanation is that SP-

containing striato-SNr neurons and enkephalin-containing striato-GPe neurons are lost at a greater rate than either SP-containing striato-SNc or SP-containing striato-GPi neurons. In end-stage HD, all classes of striatal projection neurons are affected (including striate-GPi) which may explain the bradykinesia and rigidity (Reiner *et al*., 1988; Deng *et al*., 2004). In HD, glutamic acid decarboxylase (GAD), the enzyme that is involved in GABA synthesis, is significantly decreased in GPe but not in GPi in early stages, whilst in grade 4 patients the GAD fiber depletion from both structures was much larger. (Deng *et al*., 2004)

Striatal projecting neurons and parvalbuminergic striatal interneurons degenerate during HD (Harrington and Kowall, 1991; Vonsattel and DiFiglia, 1998), whereas cholinergic striatal interneurons and striatal interneurons containing somatostatin, neuropeptide Y and/or NADPH diaphorase (or nitric oxide synthase) and medium-sized calretinergic striatal interneurons survive in the pathology (Ferrante *et al*., 1985, 1986, 1987; Fusco *et al*., 1999, Cicchetti *et al*., 2000). Multiple factors contribute to this selective vulnerability including: differential expression of Htt, changes in innervations, the extent of input from cortical or any other huntingtin-rich glutamatergic neurons or the extent to which this neurons possess certain types of glutamate receptors (Fusco *et al*., 1999).

Reactive astrocytosis (gliosis) is also a common find together with neuronal loss. Other areas of basal ganglia (especially GP and STN) also become atrophic, though less than striatum (Ross *et al*., 2001).

A 0-4 rating scale (the `Vonsattel scale') of gross and microscopic neurodegeneration, based primarily on changes in caudate and putamen (*e.g*. Figure 1.6.), has been used to semi-quantitatively describe the severity of HD. **Grade 0** appears indistinguishable from normal brains after gross examination. However, 30–40% neuronal loss can be detected in the head of caudate nucleus upon histological examination. **Grade 1** shows atrophy in the tail and in some cases the body of caudate nucleus. Neuronal loss and astrogliosis are evident in the head (50% loss), tail and, to a lesser extent, in the body of caudate nucleus. **Grade 2** is associated with gross striatal atrophy that is more pronounced than that detected in grade 1 brain. **Grade 3** displays severe gross striatal atrophy. **Grade 4** includes HD cases with severe atrophy of striatum and up to 95% neuronal loss (Vonsattel *et al*., 1985, Gil *et al*., 2008).

More severe neurodegeneration in caudate and putamen were associated with longer expanded repeat nucleotide, which is associated with a faster deterioration and greater pathological severity (Furtado *et al*., 1996).However, the degree of tissue atrophy may not be solely determined by the primary genetic abnormality (Sieradzan *et al*., 1997).

In advanced cases, total brain weight is reduced by 25-30% (Margolis *et al*., 2003).

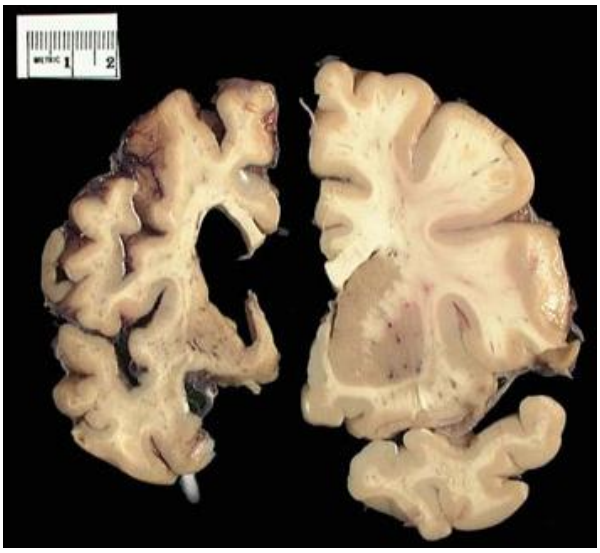

Fig. 1.6. Macroscopic image of a slice of Huntington's brain (left) and from a normal control (right). Note that striatum (caudate nucleus, putamen, and nucleus accumbens) and also cerebral cortex, on the left, are severely atrophied in Huntington's brain. Photo from the Harvard Brain Tissue Resource Center. Adapted from Http://hdroster.iu.edu/AboutHD/brainAndHD.asp

Hypothalamus is a region of the brain involved in regulation of metabolism and sleep, and includes the pituitary gland that regulates hormonal levels in the body. A substantial trophy and cell death has been described in hypothalamus from HD patients (Kremer *et al*., 1990). Cells more severely affected are located in the lateral tuberal nucleus (nucleus tuberalis lateralis, NTL) of hypothalamus. In NTL of HD patients, about 90% neuronal loss was found and the remaining neurons showed features of degeneration (Kremer *et al*., 1990). There was also astrocytosis and reduction of 40% in the number of oligodendrocytes (Kremer *et al*., 1990). This NTL vulnerability appears to be related to the high density of NMDA receptors in this nucleus (Timmers *et al*., 1996). There is also a significant loss of orexin-containing neurons in hypothalamus (Petersen *et al*., 2005)

1.1.4.1. . Formation of aggregates

Htt is a protein wih approximately 350 kDa, composed of more than 3100 aminoacids (aa). It is primarily a cytosolic protein, ubiquitously expressed in mammalian tissues, including brain

(Trottier *et al.*,1995). Cellular functions of Htt remains unclear, however it has been associated with the nucleus, endoplasmic reticulum, Golgi complex, synaptic vesicles and mitochondria (Li and Li, 2004). Some studies suggested that it has an important role during embryogenesis, being essential for gastrulation. Knockout of the gene in mouse during embryonic stage was lethal approximately at day 7.5, whilst the conditional knockout in mouse forebrain at postnatal or later embryonic stages causes a progressive neurodegenerative phenotype, suggesting a constitutive role important for neuron survival (for review, Bhide *et al*., 2006). Htt was also detected through human brain from 19th to 21st week of fetal gestation, suggesting that it may play an important constitutive role in neurons during brain development. This also suggests that the development controls heterogeneity in neuronal expression of Htt and that intraneuronal distribution of the protein may be directly correlated with neuronal maturation (for review, Bhide *et al*., 2006). Transiently knockdown of endogenous Htt by morpholino oligonucleotides in zebrafish revealed that it may be essential to development and it may be involved in normal blood function and iron utilization (Lumsden *et al*., 2007). Furthermore, Htt appears to be important during adult life. In this regard, delection of Htt gene in Drosophila showed that it may have an essential role in long-term mobility and survival of adult animals, accelerating the neurodegenerative phenotype (Zhang *et al.*, 2009). Additionally, the conditional deletion of Htt in forebrain and testis of adult mice led to degeneration of these tissues (Li and Li, 2004).

Htt interacts with a wide range of cellular proteins through multiple interaction domains. Structural analysis of Htt identified up to 36 HEAT (huntingtin, elongation factor 3, the A subunit of protein phosphatase 2A and TOR1) repeats, with approximately 40-amino acid long, composed of two hydrophobic antiparallel helices that acts as a scaffold protein.

Proposed cellular functions of Htt include endocytosis, modulation of synapse structure and synaptic transmission; transcriptional regulation (especially of brain-derived neurotrophic factor (BDNF), essential for survival of striatal neurons in HD; axonal transport of BDNF and vesicles, and anti-apoptotic activity (Ho *et al.*, 2001, Leavit *et al.*, 2001, Leavit *et al.*, 2006, Caviston and Holbaur, 2009).

HD pathogenesis has been suggested to be also related with a loss of function in wild-type Htt. This may be due to a 50% decrease in the expression of Htt and to its cleavage and sequestration into aggregates, thus impairing its neuroprotective function and culminating in neuronal dysfunction and death (Ho *et al.*, 2001). The polyglutamine repeat (polyQ) expansion promotes association with several proteins, leading to their intracellular accumulation into 5-7 μm aggregates. Formation of

such aggregates could indicate either an inability to degrade the mHtt or an overall inhibition of cellular trafficking and degradation machinery (Figure 1.7.) (Gatchel and Zoghbi, 2005).

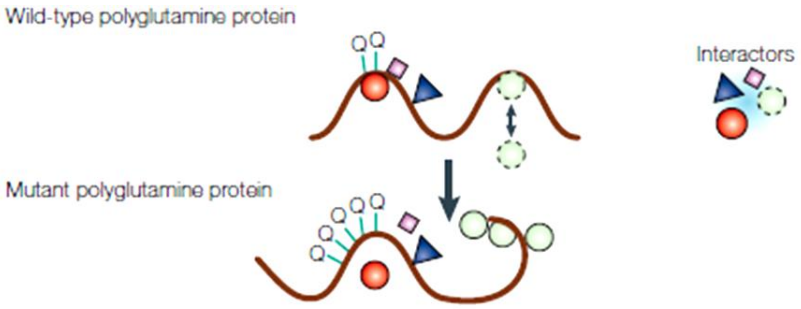

Fig. 1.7. Normal and aberrant form of polyglutamine protein. Hypothetical abnormal interactions, where some might be inappropriately enhanced and others might be lost or unchanged. [Adapted from Gatchel and Zoghbi, 2005]

Two mechanisms have been hypothesized for aggregate formation of aggregates:

- the **Polar zippers** model refers that aggregation results from multimerization by hydrogen‑bonded polar zipper. This was confirmed by the reduction of to monomeric fragments upon incubation in concentrated formic acid (Perutz *et al.*, 1994). The 40 residues threshold of polyQ has been explained by the fact that the protein sequence forms a helical fiber with 20 residues turn, and that two turns (40 residues) are required for stabilization of the helix and promotion of multimerization (for review, Hoffner *et al.*, 2007);

- **Transglutaminase‑catalyzed cross‑linking**. Transglutaminases are enzymes involved in cross-linking of glutamine residues and, thus, may also participate in the formation of aggregates. Several in vitro studies showed that depending on protein length Htt is a substrate of transglutaminase (Kahlem *et al*., 1998). Transglutaminase activity appers to be elevated in HD brain cortex and cerebellum, regions where Htt aggregates into nuclear inclusions (Karpuj *et al.*, 1999). A possible function of brain transglutaminase is stabilization of neuronal aggregates. This is corroborated by its wide distribution and activation in brain and by the occurrence of ε- (γ-glutamyl) lysine cross-linking in normal brain (Karpuj *et al.*, 1999, Hoffener *et al.*, 2007, for review, Gil and Rego, 2008).

Inclusions were found in affected areas of brain (such as cortex and caudate/putamen) but not in unaffected areas (such as cerebellum) (Hoffner *et al.*, 2005). Interestingly inclusions observed in

affected areas are limited to neurons and are not detected in glial cells (Hoffner *et al.*, 2005). In juveline form of disease, with large polyQ expansion, inclusion tend to be located in nucleous whilst in patients with the adult onset HD patients (with shorten polyQ expansion) inclusions are mostly cytoplasmatic (DiFiglia *et al*., 1997).

A study using an antibody directed against the 17 most N-terminal amino acids of Htt, showed that the frequency of nuclear inclusions (but not that of cytoplasmic inclusions) is correlated with the severity of disease, suggesting that nuclear aggregation (but not cytoplasmic aggregation) might participate in neuronal death (Hoffner *et al.*, 2005). Another study identified others aggregates located in neuropils, which are likely to correspond to dendrites, and that may contribute to neuronal death, by disturbing dendritic transport (Gutekunst *et al.*, 1999).

Several studies demonstrated that Htt fragments are more toxic to cells than full-length mHtt and that such toxicity is proportional to the size of polyQ tract, being also related to the progressive truncation of Htt (Thakur *et al*, 2009). A consequence of Htt cleavage is the release of N-terminal fragments (Htt^{NT}) containing the polyQ tract, which interacts with at least 25 proteins that can be recruited into aggregates of mHtt (Wellington *et al.*, 2003).

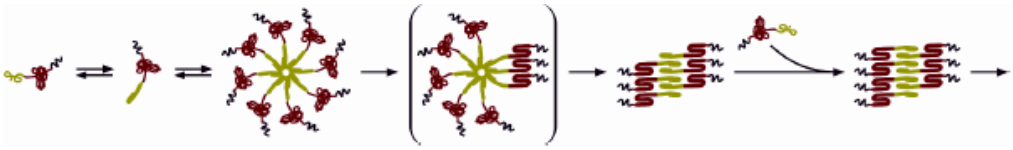

Fig. 1.8. Mechanism of Htt fragments mediated exon1 aggregation. The Htt N-terminal (Htt^{NT}) (green) unfolds in a polyQ repeat length dependent fashion and, once unfolded, self-aggregates without a nucleation barrier to form oligomers with cores comprised of Htt^{NT} and not polyQ (red). Final aggregates are rich in β-sheet, are fibrillar, and involve both Htt^{NT} and polyQ. [Adapted from Thakur at al, 2009].

In affected areas of the brain (such as cortex) normal Htt exists as a soluble monomer, but the mHtt is found in fragmented, oligomerized and polymerized forms, which can be either soluble or insoluble in water. The water-soluble forms of cortical mHtt consist of oligomerized and fragmented Htt. Soluble oligomers appear to accumulate in cortex, where they are much more abundant than the normal protein. The water-insoluble mHtt, which is mostly associated with inclusions, consists of oligomeric, polymeric and fragmented protein, establishing bonds with each other via non-covalent

bonds since they are released by formic acid. These structures are stabilized by covalent bonds since presents resistant to formic acid (Hoffner *et al.,* 2007). Some evidences have shown that this inclusions could act as neuroprotective through sequestration of toxic N-terminal fragments and oligomers of mHtt and other misfolded proteins, which would be deleterious in the soluble form (Figure 1.8.) (for review, Gil and Rego, 2008).

Accumulation of unfolded or misfolded proteins in endoplasmic reticulum (ER) could induce stress and trigger neuronal death. The apoptosis signal-regulating kinase 1 (Ask1), a MAPK kinase kinase that activates JNK pathway (c-Jun N-terminal kinases), may play a role in this process, since Ask1 is activated by ER stress and that phosphorylated Ask1 interacts with Htt fragments, allowing them to translocate into nucleus more efficiently. This interaction has a positive feedback loop, since it amplifies ER stress and may contribute to potentiate Htt toxicity (Cho *et al.,* 2009).

Activity of wild-type and mHtt can be modulated by post –translational modifications. MHtt can change post-tradutional modifications of proteins once they are formed. Several studies indicated that Htt phosphorylation at various sites is neuroprotective, by preventing cleavage of mHtt and its consequent aggregation. Activation of insulin growth factor 1 (IGF-1)/protein kinase B (Akt) pathway is protective for neurons expressing mHtt, probably due to phosphorylation of Htt on Ser421 (serine 421) (Colin *et al.,* 2008).

1.1.4.2. Intracellular mechanisms of toxicity

The gain of function of mHtt and the loss of function of wild-type Htt are potential contributors to neuronal dysfunction in HD (for review, Landles and Bates, 2004). Several processes may be involved this deregulation, as described in Figure 1.9.:

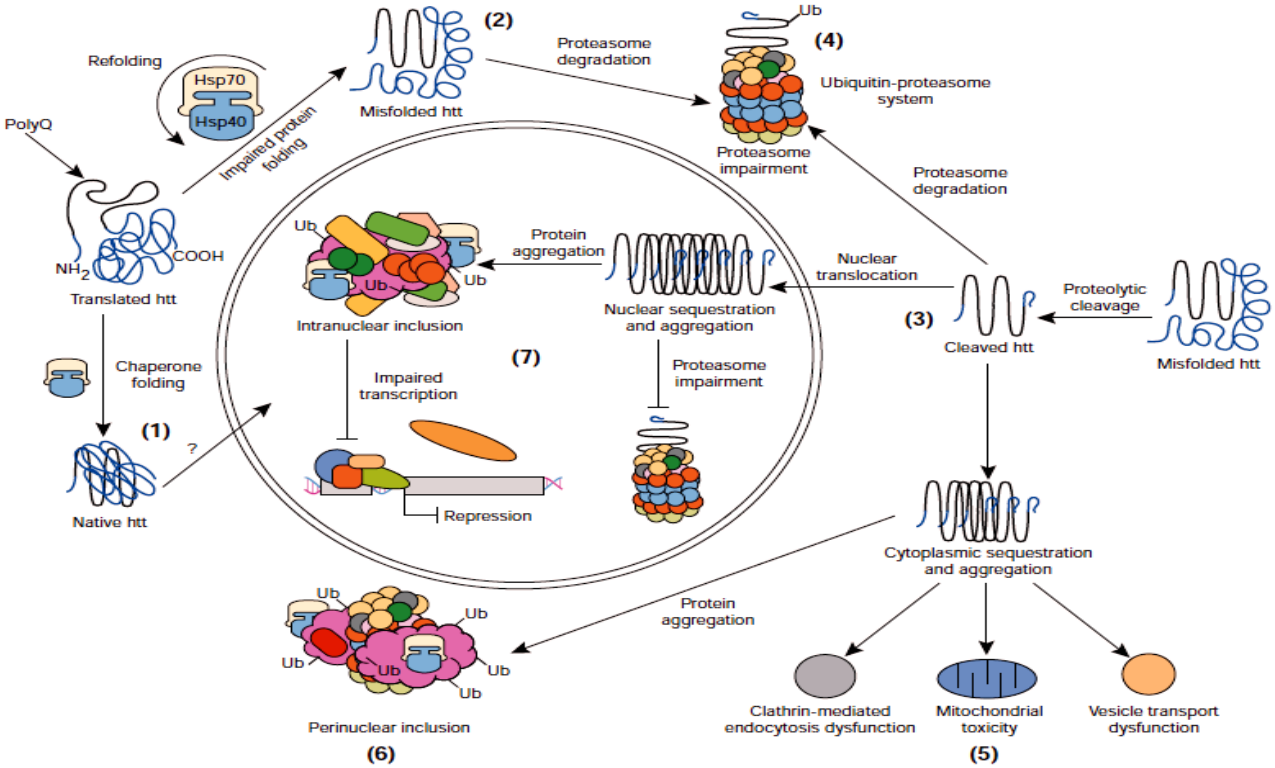

Fig. 1.9. Model for cellular pathogenesis in Huntington's disease. 1 - Molecular chaperones Hsp70 and Hsp40 promote folding of newly synthesized Htt into a native structure. Htt may be transported into nucleus and affect transcriptional regulation. Chaperones can facilitate the recognition of abnormal proteins, promoting either their refolding, or ubiquitination (Ub) and subsequent degradation by the 26S proteasome. **2-** HD mutation induces conformational changes and is likely to cause abnormal folding of Htt, which, if not corrected by chaperones, leads to accumulation of misfolded Htt in the cytoplasm. **3-** mHtt may also be proteolytically cleaved, resulting in amino-terminal fragments that form β-sheet structures. **4-** toxicity may be elicited by m full-length Htt or by cleaved N-terminal fragments, which may form soluble monomers, oligomers or large insoluble aggregates. In cytoplasm m forms of Htt may impair the ubiquitin–proteasome system (UPS), leading to accumulation of more proteins that are misfolded. **5-** These toxic proteins may also impair normal vesicle transport and clathrin-mediated endocytosis. Also, the presence of mHtt can activate proapoptotic proteins (directly or indirectly by mitochondrial damage), exacerbating cellular toxicity and other deleterious effects. **6-** In an effort to protect itself, the cell accumulates toxic fragments into ubiquitinated cytoplasmic perinuclear aggregates. **7-** In addition, mHtt can be translocated into nucleus to form nuclear inclusions, which may disrupt transcription and UPS [Adapted from Landles and Bates, 2004]

I. Protein misfolded and inhibition of protein degradation

Formation of aggregates in nucleus, cytoplasm and neurons all processes is one of the main features of HD, involving sequestration of several proteins by N-terminal fragments of mHtt (for review, Landles and Bates, 2004) Several components involved in handling and degradation of misfolded proteins (*e.g.* chaperones, ubiquitin, proteasome subunits and autophagy proteins) were found on such aggregates (Mitra *et al.,* 2009). Heat shock proteins (HSPs) may play an essential role in folding and assembly of newly synthesized proteins and in re-folding the misfolded ones and aggregation. HSP70, a molecular chaperone, is thought to bind in early stage of HD in order to maintain the protein in a soluble conformation. HSP 70 interacts with a co-chaperone protein that regulates its ATPase activity, the HSP 40 family. These chaperones also bind to misfolded proteins and are able to refold alone (Jana *et al.,* 2000). Chaperones can also re-direct these proteins to the ubiquitin-proteasone pathway and increase the expression of HSPs, which has proven to be neuroprotective. These two chaperones were found in cytoplasmic and nuclear aggregates, probably as an attempt to refold the m protein (Jana *et al.,* 2000). Chaperones were also reported to inhibit caspase-3 and 9 activities and to improve cell viability independently of aggregate formation (Zhou *et al.,* 2001).

mHtt was shown to interact with numerous transcriptional factors, such as NF-Y, which has been reported to regulate HSP70 transcription, resulting in an overall reduction of HSP 70 gene expression (Yamanaka *et al.,* 2008).

The ubiquitin-proteosome system (UPS) is another neuroprotective mechanism that prevents accumulation of misfolded proteins, by degrading them. *In vivo* studies have shown that UPS activity is impaired and some components of proteosome are sequestered into aggregates (Wang *et al.,* 2008). MHtt can be ubiquitinated, itself, which may represent an attempt to eliminate the aggregates (Mitra and Finkbeiner, 2008). However, several hypotheses have been proposed to explain such impairment: 1) mHtt could be retained in proteolytic core and impair proteasome activity; 2) mHtt aggregation may impair proteasome or 3) for the proteasome regulatory complex to unfold mHtt and present it to the core catalytic subunits for proteolysis (Mitra and Finkbeiner, 2008). In this regard, it has been suggested that HD could be a proteasomal storage disease (Goellner and Rechsteiner, 2003).

A recent study used mass-spectrometry-based methods to quantify polyubiquitin chains from transgenic mouse and knock-in models demonstrating that the abundance of lysine 48-linked polyubiquitin chains could be a faithful endogenous biomarker of UPS function (Bennett *et al.,*

2007). These chains where shown to accumulate early in brains of mice and humans with HD showing that UPS dysfunction is a consistent feature of HD pathology (Bennett *et al.,* 2007).

While UPS mainly degrades short nuclear and cytosolic proteins, bulk degradation of cytoplasmic proteins or organelles is largely mediated by macroautophagy (also known as autophagy) (for review Chu, 2006). Increased autophagy was previously found in HD, probably as a response to reduce the toxicity induced by the aggregates (Sapp et al., 1997).

II. Caspase activation

Proteases (including caspases, calpains and aspartyl endopeptidades) are involved in cleavage of Htt within the N-terminal domain (Graham *et al.,* 2006). Several studies demonstrated that Htt is a caspase substrate with defined sites for caspase-3 at amino acids 513 and 552, for caspase-2 at amino acid 552, and for caspase-6 at amino acid 586 (Wellington *et al.,* 1998, 2000). Two caspase-3 consensus sites at amino acids 530 and 589 that appear to be silent have been also decribed (Graham *et al.,* 2006). Htt is cleaved by caspase 3 and 6 *in vitro*, and caspase-3-cleaved Htt fragments have been identified in HD brain, prior to the clinical onset. This suggests that N-terminal Htt fragments may play a role in HD pathogenesis (Graham *et al.,* 2006). Both wild-type and mHtt can be cleaved by proteases, but fragments generated from wild-type Htt appear to be more efficiently cleared through the ubiquitin–proteasome pathway (Wellington *et al*., 2002). Such fragments were mainly detected in cytoplasm, which may indicate that this precedes nuclear uptake of N-terminal Htt fragments (Wellington *et al*., 2002).

MHtt can also reduce the ability of Htt to bind and inhibit active caspase-3 and to bind HIP1 (Htt interaction –protein 1), which is then free to associate with HIPP1 (HIP1-protein interactor) and activate caspase-8, an initiator caspase involved in the apoptotic cascade (for review, Gil and Rego, 2008, a review). In FVB-YAC128 mice expressing full-length mHtt, the inhibiting of caspase-6 (but not caspase-3) was shown to protect loss against striatal volume and neuronal loss, suggesting that caspase-6-mediated proteolysis of mHtt (586 aa), generating a toxic fragment and mediates excitotoxic stress. Cleavage of Htt could be an 'initiating' factor for neuronal dysfunction, by generating toxic fragments, altering cellular trafficking and gene expression patterns and activating cell death pathways via altered interaction with Htt-associated proteins (Figure. 1.10.) (Wellington *et al.,* 2003). Htt proteolysis could also act as a feed-forward loop, in which cleavage may occur prior to the onset of neurodegeneration in HD, and initiate or exacerbate progression towards activation of cell death proteases and subsequent cell death (Wellington *et al.,* 2003).

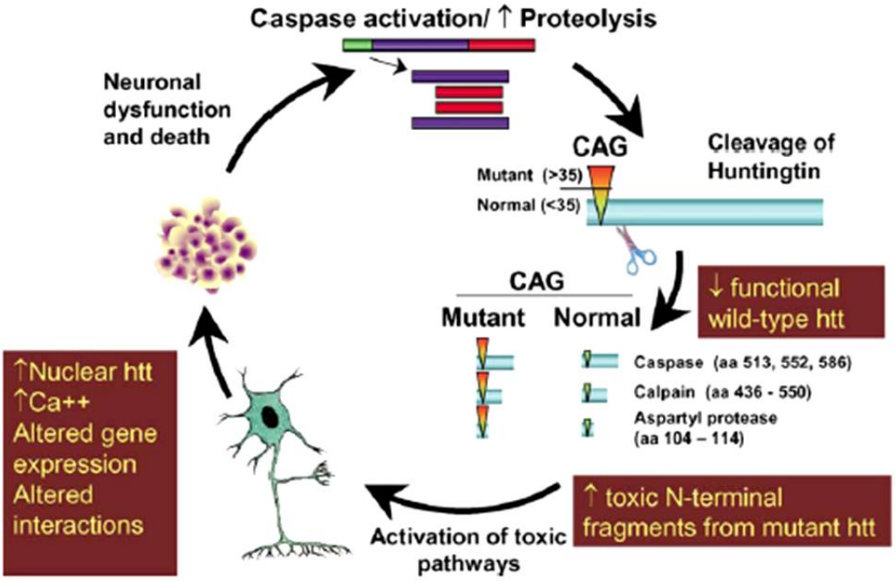

Fig. 1.10. The toxic fragment hypothesis. Cleavage of Htt generates toxic N-terminal fragments that, when containing expanded polyQ tracts, are not efficiently degraded and accumulate within cells. Resulting fragments initiate several changes in the cell. (Adapted from Wellington *et al.*, 2003).

Calpains are a family of Ca^{2+}-dependent intracellular cysteine proteases, activated by elevated intracellular calcium levels, which cleave Htt between amino acids 437 and 540 an area that overlaps with caspase cleavage sites in the protein (amino acids 518–586) (Wellington *et al.,* 2003).

III. Transcription deregulation

It has been proposed that mHtt interacts with several transcriptional factors recruiting them into the aggregates and inhibiting their activity (for review, Bithell *et al.,* 2009). Important transcriptional factors (*e.g.* CREB [cyclic-adenosine monophosphate (cAMP) response element (CRE)] binding protein (CBP) (Steffan *et al.,* 2000; Nucifora *et al.,* 2001), specific protein-1 (SP1) (Li *et al.,* 2002), TATA-binding protein (TBP), TBP-associated factor TAFII130 (Dunah *et al.,* 2002) and the pro-apoptotic transcription factor p53) directly interact with mHtt (Steffan *et al.,* 2000). CBP, with a polyQ stretch, is sequestrated into mHtt aggregates, suppressing CREB-mediated CRE transcription (Steffan *et al.,* 2000). TBP, also containing a polyQ stretch, and was shown in an *in vivo* study to be incorporated into mHtt aggregates and to suppress its DNA binding by mHtt (Steffan *et al.,* 2000). SP1, which binds to glutamine-rich region in certain promoters and activates

transcription of the corresponding genes and TAFII130 interacts with a soluble form of mHtt, suppressing of SP1 transcriptional activity and finally downregulating dopamine D2 or nerve growth factor receptor (Steffan *et al.,* 2000). p53 is incorporated into mHtt aggregates via its SH3 sequences, leading to repression of p53-mediated transcription (Steffan *et al.,* 2000).

Interaction of mHtt fragments with transcriptional factors is sufficient for transcriptional deregulation *in vivo* suggesting a model whereby mHtt interacts directly with DNA, altering its conformation and transcription factor binding and ultimately leading to transcriptional deregulation (Benn *et al.,* 2008). Benn *et al.* (2008) observed that both wild-type and mHtt occupy gene promoters *in vivo* and proposed the enhanced genomic DNA binding by mHtt, (facilitated by its nuclear-localization) alters DNA conformation and subsequent binding of transcription factors, disrupting normal control of mRNA expression at an early time point in HD pathogenesis. Several transcription factors that interact with the mutant protein have acetyltransferase activity that may impair gene expression, by altering histone acetylation levels. Hypoacetylation has been linked to repression of gene activity (Sadri-Vakili *et al.,* 2006)

mHtt can also inhibit gene expression in the cytosol (Zuccato *et al.,* 2003). Wild-type Htt was found to interact with the repressor element-1 transcription factor (REST) in cytoplasm. REST associates with neuron restrictive silencer factor (NRSF) to affect nuclear transcription of neuronal genes, including that of BDNF. This interaction REST– NRSF could prevent their entry to nucleus and thus reduce their suppression of gene expression. However mHtt bind weakly with REST–NRSE, leading to increased accumulation of REST–NRSF in nucleus and subsequent inhibition of BDNF and other genes expression (Zuccato *et al.,* 2003).

IV. Disruption of axonal transport

Several Htt-binding cytoplasmic proteins are involved in vesicle trafficking and intracellular transport. A particular protein, HAP 1, was proposed to facilitate the interaction with microtubule motor proteins, forming a complex with kinesin (plus-end directed microtubule motor protein) and with $p150^{Glued}$ subunit of dynactin (Caviston *et al.,* 2007). A study demonstrated a co-precipitation of a complex that includes cytoplasmic dynein, dynactin, Htt, kinesin and HAP1 (Caviston *et al.,* 2007). HAP1 is a multidomain protein with versatile functions that also interacts with HGS, which in turn participates in endocytosis of the epidermal growth factor (EGF) receptor (Gauthier *et al.,* 2004). HAP1 was recently found to interact with the type 1 inositol (1,4,5)-trisphosphate receptor (IP31), forming an IP31–HAP1A–Htt ternary complex in which the mHtt enhances the sensitivity of IP31 to

inositol (1,4,5)-trisphosphate (for review, Li and Li., 2004). HAP1 interacts with NeuroD (a transcription factor important for neuronal development and survival) and Htt interacts with NeuroD via HAP1 (for review, Gil and Rego, 2008). Htt has also been linked to actin-based motors through optineurin, a protein that links myosin VI to Golgi membranes (Caviston *et al.,* 2007). A neurotrophic factor essential for neuronal survival, BDNF, is decreased in striatal neurons. BDNF is secreted by cortical neurons, delivered by axonal transport and re-endocyted by striatal neurons (Gauthier *et al.,* 2004). In several studies, it was shown that mHtt plays an important role such depletion, as a consequence of defective axonal trafficking (Gauthier *et al.,* 2004). A study demonstrated an increased association of polyQ-Htt to HAP1 and $p150^{Glued}$, leading to the depletion of HAP1, $p150^{Glued}$, dynein IC (intermediate chain), and kinesin HC from microtubules (Gauthier *et al.,* 2004). This occurs mainly in the early stage of disease, while in later stages neuritic aggregates accumulate and contribute to reduce axonal transport (Gauthier *et al.,* 2004)

V. Synaptic dysfunction

Interactions of mHtt with cytoplasmic proteins have been involved in synaptic dysfunction, either by impairment of axonal transport or sequestration of synaptic vesicles or proteins necessary for endocytosis and recycling (*e.g.* membrane receptors) (Trushina *et al.,* 2006). Inhibition of endocytosis occurs through a non-clathrin, caveolar related pathway (Trushina *et al.,* 2006). A recent study revealed that mHtt leads to accumulation of intracellular cholesterol, which is essential to promote synapse formation and maintenance membrane integrity in CNS (central nervous system) neurons (Trushina *et al.,* 2006).

Another Htt-interacting protein is the neurospecific phosphoprotein PACSIN 1/syndapin, which is located along neurites and within synaptic boutons and has been implicated in synaptic vesicle recycling (Modregger *et al.,* 2002). Interaction through C-terminal SH3 domain with mHtt leads to re-localization of PACSIN 1 away from varicosities towards neuronal cell body (Modregger *et al.,* 2002). SH3-containing proteins, binding partners for synaptojanin and dynamin I, play a major role in signal transduction from membrane receptors and in regulation of exo/endocytic cycle of synaptic vesicles (Sittler *et al.,* 1998). MHtt was also found to bind to this domain and may contribute to neuronal cell death (Sittler *et al.,* 1998). Another example of loss of function is HIP14 (a neuronal protein that is located mainly in Golgi apparatus and cytoplasmic vesicles) that interacts strongly with wild-type Htt but weakly with the mutant protein and may compromise intracellular traffic (Singaraja *et al,* 2002)

Several proteins involved in exocytosis are decreased in HD, including complexin II (Smith *et al.*, 2005). Complexin II interacts with the soluble N-ethylmaleimide-sensitive fusion protein attachment protein receptor (SNARE) complex (involved in neurotransmitter release and regulation of membrane fusion between the synaptic vesicle and the presynaptic plasma membrane) (Smith *et al.*, 2005). Another protein whose levels are decrease is rabphilin 3A that is involved in priming and docking of vesicles to the plasma membrane (Smith *et al.*, 2005).

Excitotoxicity induced by glutamate has been implicated as one of the main causes of neuropathology of HD (Fan and Raymond, 2007). R6 transgenic mice have an increased release and a decreased clearance of glutamate by the glial cell glutamate transporter GLT1 with subsequent sustained glutamate stimulation of striatal neurons (Smith *et al.*, 2005). Neurons from mice R6/2 were shown to have increased responses of NMDA and decreased Mg^{2+} sensitivity, suggesting that NMDA receptor alterations may occur very early in development and that constitutively abnormal NMDA receptors with enhanced response may be present (Starling *et al.*, 2005). MHtt facilitates activity of NR2B subtype of NMDARs and InsP3R1, causing influx of Ca^{2+} (Tang *et al*., 2004). Activation of glutamatergic receptors alters Ca^{2+} homeostasis, which in turn affects downstream pathways and initiate second messenger cascades (Fan and Raymond, 2007). When buffering capacity is compromised, activation of catabolic enzymes (such as nucleases, proteases and phospholipases) as well as generation of free radicals and induction of mitochondrial damage can occur (Fan and Raymond, 2007).

Metabotropic glutamate receptors (mGluR) (*e.g.* mGluR1, mGluR2 and mGluR3) and ionotropic receptors (3-hydroxy-5-methyl-4-propionate (AMPA) and kainate receptors (KA)) as well as D1 and D2 dopamine (DA) receptors were also found to be decreased or with decreased binding activity in R6／2 mouse model (for review, Gil and Rego, 2008).

Interestingly, normal Htt associates with postsynaptic density 95 (PSD-95), a scaffold protein that causes clustering and activation of receptors in postsynaptic membrane. Decreased interaction of mHtt with PSD-95 may activate NMDARs (Li and Li, 2004).

VI. Mitochondrial dysfunction

Defects in mitochondrial respiratory chain in caudate/putamen of HD patients have been reported include severe reduction in activity of complex II/III and milder decrease of complex IV activity (Sawa *et al*., 1999). Transcriptional impairments produced by mHtt could lead to disruption of Ca^{2+} homeostasis, which may further reduce CREB-dependent expression of mitochondrial

oxidative phosphorylation proteins (Gopalakrishnan and Scarpulla, 1999). Mitochondrial respiration and ATP production were found to be significantly impaired in striatal cells expressing mHtt. Moreover, mHtt can also affect mitochondrial function by inhibiting expression of PGC-1α (peroxisome proliferator-activated receptor gamma co-activator 1-alpha), a transcriptional factor required for expression of numerous genes that promote the detoxification of reactive oxygen species (ROS) and prevent oxidative stress (Quintanilla and Johnson, 2009, for review). Tang *et al.* (2004) propose that such vulnerability could arise from glutamate released by corticostriatal projection neurons, stimulating NR1/NR2B-composed NMDARs and mGluR5 receptors. Activation of NR1/NR2B NMDARs leads to Ca^{2+} influx and activation of mGluR5 receptors through the production of InsP3 and Ca^{2+} release via InsP3R1. Indeed, mHtt sensitizes InsP3R1 to activation by InsP3, stimulating NR1/NR2B NMDAR activity, and directly destabilizing mitochondrial Ca^{2+} handling. As a result, an abnormal Ca^{2+} response in MSN occurs, leading to an overload in cytosolic Ca^{2+}, which is then taken into mitochondria via Ca^{2+} uniporter/channel. If this occurs continuously, changes storage capacity limit of mitochondrial Ca^{2+} can lead to opening of mPTP (mitochondrial permeability transition pore), release of cytochrome *c* into cytosol, and activation of caspase-mediated intrinsic apoptotic program (Oliveira *et al.*, 2007). MHtt can also interact directly with outer mitochondrial membrane increasing the sensitivity of the mPTP to Ca^{2+} or other apoptotic stimuli and also the aggregates could impair mitochondrial movements along neuronal processes (for review, Damiano *et al.*, 2010)

Weydt *et al*. (2006) found a decreased number of functional mitochondria, ATP/ADP and expression of PGC-1α target genes (involved in energy production) in brown adipose tissue from HD mice (N171-82Q mice). This suggests that inhibition of PGC-1α (usually involved in adaptive thermogenesis) may cause a global defect in mitochondrial function in HD mice. The authors also showed that these HD mice develop hypothermia associated with impaired activation of brown adipose tissue-mediated thermogenesis, supporting the hypothesis that impaired PGC-1α activity links neurodegeneration-associated mitochondrial dysfunction to thermoregulatory and metabolic defects in HD (Weydt et al., 2006).

Normal average rectal temperature in mice is 37.5^{o}C, but it depends on circadian fluctuations and is highly decreased during fasting (especially at noon) (Swoap in Howard Hughes Medical Institute, 2010) (Figure 1.11.).

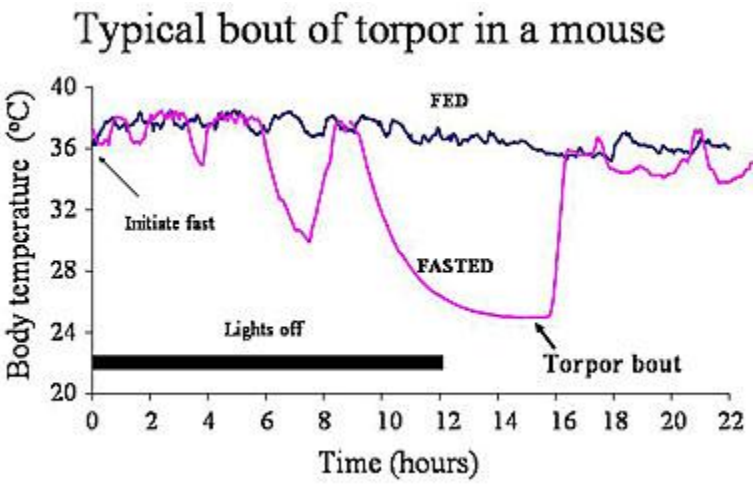

Fig.1.11. Daily body temperature fluctuations in a mouse under fed and torpor conditions.

[Obtained from Http://www.hhmi.org/news/popups/images/20060131_graph.jpg, Steven J. Swoap, Howard Hughes Medical Institute]

1.2. Metabolic changes in HD

1.2.1. Glucose metabolism

Under normal conditions glucose is the main substrate for cerebral energy metabolism. But in particular circumstances, the brain also consumes monocarboxylic acids, including lactate and ketone bodies, acetoacetate and β-hydroxybutyrate (Owen *et al.*, 1967). In glycolysis, glucose is degraded to pyruvate and then to lactate (Figure 1.12.). This process is not very energy-efficient, resulting only in the production of 2 mol of ATP/mol of glucose and in regeneration of reducing equivalents (the oxidized form of nicotinamide-adenine dinucleotide, NAD^+). Then, pyruvate can enter the tricarboxylic acid cycle (or Krebs cycle) and produce 34 mol of ATP/mol of glucose via mitochondrial oxidative phosphorylation having a potential to generate a total of 38 mol of ATP/mol of glucose (Guyton and Hall, 1998).

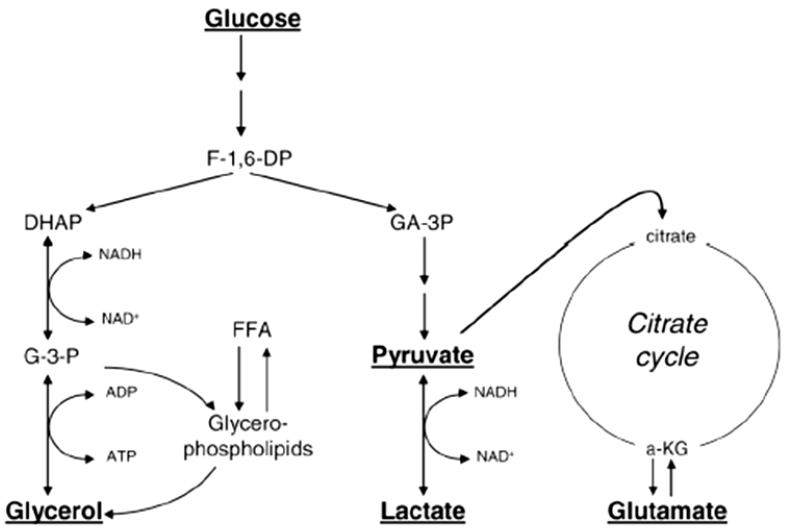

Fig. 1.12. Glycolytic pathway leading to phospholipid formation, lactate and pyruvate a substrate to the citric acid cycle. F-1,6-DP, fructose-1,6-diposphate; DHAP, dihydroxyacetone-phosphate; GA-3P, glyceraldehyde-3-phosphate; G-3-P, glycerol-3-phosphate; FFA, free fatty acids; La/py, lactate/pyruvate; a-KG, α-ketoglutarate. (Adapted from Nordström, 2008)

In a recent study, glucose metabolism was found to be significantly decreased in striatum and temporal and frontal cortical lobes, in both preclinical and affected HD patients, with marked striatal hypometabolism is seen in later stages of disease reflecting neuronal atrophy (Ma *et al.*, 2007). Thalamic hypermetabolism and cortical hypometabolism and hypoperfusion have also been detected

in early stage of symptomatic HD patients with Positrons Emission Tomography or Single Photon Emission Computed Tomography (Ma *et al.*, 2007).

As it was described previously mHtt and its fragments can interfere with energy production, through interaction with a variety of key proteins involved in energy metabolism. MHtt has been found to interact with a important enzyme involved in glycolysis GAPDH (glyceraldehyde-3-phosphate dehydrogenase), partially inhibiting its activity in a disease progression dependent manner and as more fragments interact with GAPDH, causing a significant decrease in ATP production culminating in cell death (Wu *et al.*, 2007).

MHtt is also known to interfere with oxidative phosphorylation, the final step in ATP production pathway. Defects in HD respiratory chain have been observed, since mHtt can dramatically decrease the activity of complex II/III and mildly complex IV. This could be probably due a preferential decrease of respiratory chain enzymes, in particular complex II (SDH/II - succinate dehydrogenase) and to a lesser extend cytochrome c oxido-reductase (IV) (for review, Damiano *et al.*, 2010).

It has been widely described that HD patients have increased brain lactate levels, suggesting that damage to mitochondria and impaired energy metabolism may occur in the disease, leading to conversion of pyruvate in lactate to generate ATP (Koroshetz *et al.*, 1997). Although glucose is the primary energy source for neurons and astrocytes, the first can utilize glial-produced lactate as an additional energy substrate under abnormal conditions (Pellerin L and Magistretti, 1994). Increased lactate reflects metabolic and energy impairment, resulting in tissue acidosis which in turn induce glial and neuronal cell swelling (Koroshetz *et al.*, 1997). It has been described that pyruvate concentrations are significantly lower in HD patients group, which may also increase the L/P ratio (Koroshetz *et al.*, 1997)

A condition unexpected and often found in HD patients is weight loss and muscle wasting (Gaba *et al*., 2005). The disease is often accompanied by considerable weight loss, particularly on its final stages, which seems directly associated with the number of CAG repeats (Aziz *et al.*, 2008). Patients with higher body mass index were linked with slower progression of HD (Myers *et al.*, 1991). HD patients are either underweight (Djoussé *et al.*, 2002), or tend to lose weight during the course of their illness, eventually becoming cachectic in end-stage (Aziz *et al.*, 2008). Although the reason for weight loss remains debatable, it seems to be unrelated to anorexia-mediated decrease food intake, since these patients normally have increase caloric uptake (Trejo *et al.*, 2004). Some studies referred increased motor activity could be involved in weight loss (Pratley *et al.*, 2000),

whilst others referred a hypermetabolic state, leading to a negative energy balance (Aziz *et al.*, 2008; Goodman *et al.*, 2008). One study reported that total energy expenditure was 11% higher in HD patients (Gaba *et al.*, 2005). The majority of presymptomatic HD patients also present an altered metabolic profile which may therefore represent an early step in HD pathogenesis and general metabolic derangement (Gaba *et al.*, 2005).

1.2.2. Diabetes mellitus in HD

When glucose metabolism is impaired and glucose uptake by cells is reduced, blood glucose levels rise. If this occur chronically a metabolic disease, Diabetes Mellitus, can arise (WHO, 2006). The most common Diabetes mellitus forms are type I and type II. Type I diabetes is characterized by loss of insulin-producing *β*-cells in pancreatic islets of Langerhans leading to insulin deficiency. In type II diabetes insulin resistance is the main characteristic and, initially, there is no reduction in insulin secretion, but a deficient response to insulin (James and Piper, 1994).

In HD there is some controversy on the prevalence of diabetes. The first paper describing a higher prevalence of diabetes in HD was Podolsky *et al.* (1972) in which 50% of the patients studied had impaired carbohydrate metabolism, probably due to decreased insulin secretion. In 1985, Ferrer studied 620 probands with HD and found that 65 of them (10.5%) had diabetes, suggesting that HD patients had 7 times more probability of have diabetes. A more recent study, focused on changes in insulin sensitivity and insulin resistance, major determinants of glucose homeostasis, in a group of consecutive normoglycemic patients with HD, showed impairment in insulin secretion capacity, accompanied by simultaneous decrease in insulin sensitivity and an increase in the insulin resistance (Lalić *et al.*, 2008). A possible explanation may involve mHtt inclusions (expressed also in pancreatic *β*-cells) that become dysfunctional and leads to diabetes 2 (Andreassen *et al.*, 2002). However, this relation was not found in another study, perhaps because the patients studied had different anthropometric features (Boesgaard *et al*., 2009). Moreover, mice models were also shown to develop glucose intolerance and glycosuria (R6/2 (Bjőrkqvist *et al.*, 2005); R6/1 transgenic mouse (Josefsen *et al.*, 2008) and HD-N171-82Q mice (Schilling *et al*., 1999)). Recently, Hunt *et al.* (2005) found that 70 % of R6/2 mouse at 14 weeks of age develop diabetes and its severity was associated with progressive formation of ubiquitinated inclusions in pancreatic *β*-cells. Accumulation of such aggregates was associated with selective disruption in expression of transcription factors essential for glucose-responsive insulin gene expression leading to in impairment of insulin release rather than insulin resistance (Hunt *et al.*, 2005). Bjőrkqvist *et al.* (2005) identified two separate pathological

processes that may be responsible for diabetes in R6/2 mice: impaired *β*-cell replication (resulting in deficient *β*-cell mass (~35%) most likely due to impaired regeneration of islet cells) and a reduction of insulin-containing secretory granules (abrogating stimulated hormone secretion). R6/1 mice, carrier of a shorter CAG repeat, although not diabetic, shows impaired glucose tolerance (Josefsen *et al.*, 2008).

1.3. *In vivo* models of HD

The most reliable models reproduce neuropathological hallmarks such as degeneration of GABAergic medium spiny neurons at an early stage and cortical loss in advanced conditions and especially the phenotype of the disease (for review, Rubinsztein, 2002). Two categories of animal models were generated: the non-genetic and the genetic ones. Non genetics animal models were the only available before discovery of gene mutation and used excitotoxic mechanisms or mitochondrial dysfunction to induce neurodegeneration, primarily at striatum. Quinolinic acid (QA) and kainic acid (KA) are the most commonly used excitotoxic agents, acting as agonists of NMDA receptors, whereas 3-nitropropionic acid (3-NP) and malonic acid (MA) induce cell death in striatal neurons through inhibition of mitochondrial complex II (succinate dehydrogenase), disrupting mitochondrial electron transport chain with subsequent impairment in ATP synthesis (for review, Ferrante, 2009).

Recently, genetic engineering led to the production of transgenic animals, inserting genetic material in the host genome or into the Htt gene locus, resulting in knock–in models. In HD cases, the material inserted comprised protein-coding region exon -1 (which expresses truncated protein) or the full length Htt gene, expressing the entire protein (for review, Ferrante, 2009). The most widely used animals are rodents and, recently, also non-human primates (Yang *et al.*, 2008), but other non-mammalian animals exist (such as *Caenorhabditis elegans*, *Drosophila melanogaster* and *Zebrafish*) (Fecke *et al*., 2009). These models are simple and have a rapid development, allowing high-throughoutput testing of novel therapeutic compounds and strategies (Fecke *et al*., 2009).

Currently, a wide range of models is available, differing in background, fragment/full-length gene, CAG repeat length, promoter and endogenous expression of transgene. Those particular characteristics of each model influence the disease neuropathology and phenotype (for review, Ferrante, 2009). Frequently there is an inverse correlation between the severity of disease/symptoms, lifespan and mHtt expression and transgenes length (for review, Ferrante, 2009). The full-length models are genetically more accurate, but the fragment models have a rapidly disease progression

with a robust phenotype, well-defined behavioural and neuropathological findings and premature death between 13 and 18 weeks of age (*e.g.* Carter *et al*., 2000).

For the purpose of this work, in the next sub-section we will focus on the transgenic models expressing full-length mHtt.

1.3.1. Full-length human HD gene transgenic mouse models

In 1999 Hayden and colleagues developed a YAC (yeast artificial chromosome) transgenic mouse using a YAC vector system to express the entire human Htt gene under control of the human Htt promoter. YAC mouse strains contain either 72 or 128 CAG repeats. The mice with 72 expansions show a selective degeneration of medium spiny neurons in the lateral striatum with the translocation of N-terminal Htt generation specifically in the striatum (Hodgson *et al*., 1999). The YAC128 has an increased size of CAG expansion of 128 CAG and in 2003 Slow *et al.* characterize the natural history of disease in these mice. Motor abnormalities and age-dependent brain atrophy were found. In early stages of disease the mice develops a hyperkinetic phenotype manifest at 3 months of age, followed by a progressive motor deficit on the rotarod at 6 months with progression to hypokinesis by 12 months of age. There is a high correlation between motor abnormalities and striatal atrophy, which is evidently at 9 months of age, and develops into cortical atrophy at 12 months and significant decrease (~15%) in striatal neurons accompanied by a decrease in striatal cell surface area.

The motor deficit at 6 months correlates well with evident neuronal loss at 12 months, suggesting that early motor dysfunction might be an indicator of the severity of the extent of dysfunction of striatal neurons YAC128 mice also develop mild cognitive deficits, which precedes the onset of motor abnormalities and progressively deteriorate with age (Van Raamsdonk *et al.*, 2007). Htt inclusions appear latter to behavioral and neuropathological changes associated with neuronal death, at 18-month-old, presupposing that inclusions are not the main cause to neurons loss. Excitotoxicity was described has the most important mechanism responsible for cell death in which disturbed neuronal Ca^{2+} signaling is involved. An increased NMDAR-mediated current in the MSN cultured from the YAC128 model corroborates this idea (Shehadeh *et al.,* 2006, Van Raamsdonk *et al.*, 2007; Zhang *et al.,* 2008). This susceptibility to neuronal excitability is age-dependent in YAC128 which may be conditioned by background strain since FVB/N WT mice have an age-dependent decrease in susceptibility to excitotoxic stress probably resulting from morphological changes including decreases in synaptic density, spine density and loss of distal dendritic segments

(Graham *et al.,* 2009). Body weight in YAC128 mouse line is increased at 2 month of age (Van Raamsdonk *et al.,* 2007) represented by an increase in both fat mass and fat-free mass influenced by Htt which modulates the IGF-1 pathway (Pouladi *et al.,* 2010).

Table IV- Comparison of the YAC72 and YAC128 mouse models of Huntington disease.

	YAC72	YAC128
Promoter	Human HD gene promoter	Human HD gene promoter
CAG repeat length	72	120
Protein expression levels	Line 2511: ~33% endogenous line 44: ~133% endogenous	Line 53: ~75% endogenous
Behaviour: movement		
Rotarod	No difference (line 2511), deficit at 12 months (line 44)	Deficit at 4 months
Open field activity	Hyperactive at 7–9 months (line 2511), no difference (line 44)	Hyperactive at 2 months, hypoactive at 8–12 months
Gait	Decreased stride length (line 44)	Not assessed
Behaviour: cognition		
Motor learning on rotarod	Not assessed	Deficit at 2 months
Pre-pulse inhibition	Not assessed	Deficit at 12 months
Linear swimming test	No difference (line 44)	Deficit at 8 months
Swimming T-maze test	Not assessed	Deficit at 2 months (reversal)
Open field habituation	Not assessed	Deficit at 9 months
Physical measurements		
Body weight	Decreased (line 44)	Increased at 2 months
Neuropathology		
Striatal volume	Decreased at 10 months (line 44)	Decreased at 9 months
Striatal neuronal counts	No difference (line 44)	Decreased at 12 months
Striatal neuronal cross-sectional area	Not assessed	Decreased at 12 months
Striatal DARPP-32 expression	Not assessed	Decreased at 12 months
Cortical volume	Not assessed	Decreased at 12 months
Volume of globus pallidus	Not assessed	Decreased at 12 months
Nuclear EM48 staining	Present at 12 months, selectively in striatum (line 2511)	Present at 1-2 months, selectively in striatum
Macroaggregates by light microscopy	None at 12 months	Rare at 12 months, present at 18 months
Dark cell degeneration	Present at 12 months (line 2511)	Not assessed

[Adapted from Van Raamsdonk *et al*., 2007]

YAC128 mice were initially generated on the FVB/N background strain based on its advantages in generating transgenic mice and its known susceptibility to excitotoxicity (Taketo *et al.*, 1991). This strain has a particular characteristic that makes it attractive to create HD transgenic mice, since it exhibits a high degree of neuronal loss when exposed to excitotoxic stress after injection of kainic acid or quinolinic acid, in an age dependent manner, not experienced in other HD transgenic strains (Schauwecker *et al*., 2002, Graham *et al*., 2009). YAC128 are useful to assess therapeutical interventions, since it reproduces well the phenotype of disease in humans.

1.4. Hypothesis and aim of this thesis

As described above, HD is a multifactorial neurodegenerative disease, characterized by cognitive deficit, motor abnormalities, weight loss, endocrine changes (Foroud *et al.,* 1999). The later may include impaired carbohydrate metabolism, diabetes and changes in insulin sensitivity and insulin resistance, which are major determinants of glucose homeostasis (Podolsky *et al.,* 1997, Lalić *et al.,* 2008). Although such evidences remain controversial in human HD patients, they have been well characterized in the R6/2 mouse model (Bjőrkqvist *et al.,* 2005), expressing the exon-1 of human mHtt. However, to our knowledge, no studies have been performed in HD animal models expressing full-length mHtt.

The YAC128 mouse expresses full-length mHtt with 128 glutamines and present a phenotype and history course similar to HD patients, namely the motor impairment, cognitive decline, striatal neuronal loss and metabolic dysregulation (Slow *et al*., 2003, Van Raamsdonk *et al.,* 2007). However, and in contrast to HD patients, these mice show increased body weight (Slow *et al*., 2003, Van Raamsdonk *et al.,* 2007; Pouladi *et al*., 2010). Furthermore, the YAC128 transgenic mice have been created in a background strain susceptible to metabolic deregulation and insulin resistance, the FVB strain (*e.g.* Junghyo *et al*., 2009). Under this perspective, we hypothesized that expression of full-length mHtt in an hyperglycemic background (conferred by the FVB strain) could aggravate motor impairment, changes in body weight and metabolic deregulation and possibly insulin resistance.

Therefore, the aim of the present study was to evaluate the effect of hyperglycemic background on peripheral and central metabolic parameters in an *in vivo* rodent model of HD expressing full-length mHtt. In this regard, we used hyperglycemic 6 month-old YAC128 mice *versus* age-matched WT (FVB/N) mice littermates.

CHAPTER II

MATERIALS AND METHODS

2.1. Materials

Avertin (Tribromoethanol) syringes 1ml Plastipak® from BD (Franklin Lakes, USA). Needles 1,1x40 mm, paraformaldehyde 4% (0.1 M PBS at pH 7.4), Sodium Azide, Eppendorf from Bioplastics BV, Netherlands, Centrifuge 5417C (Eppendorff®). Digital glucometer, The OneTouch® Ultra®, and compatible stripes were from Johnson & Johnson Company (Milpitas, CA, USA). High-precision electronic weighing scale Kern 440-47 N® was from Kern & Sohn GmbH (Balingen, Germany) and the digital thermometer, Ved digital II® from Artsana S.P.A. (Grandate, Italy). Rotarod and Open Field apparatus were from Panlab® (Barcelona, Spain). PCR reagents, such as MasterMix, Buffer, $MgCl_2$, and Taq Polymerase, and also proteinase K, DNA Ladder 100 bp and DNA Loading Dye were purchased to Invitrogen® (Carlsbad, CA, USA). *D*-Glucose and human recombinant insulin was from Sigma-Aldrich Co (St. Luis, MO, USA) were reconstituted in MiliQ water. Insulin (Mouse) Elisa kit was obtained from ALPCO (Salem, USA). Quantikine® Mouse/Rat IGF-I Immunoassay was purchased to R&D Systems, Inc. (Minneapolis, USA). Pyruvate Assay Kit (ab65342) and Lactate Assay Kit (ab65331) were both obtained from Abcam (Cambridge, UK). Methylene Blue (1%). HPLC column Lichrospher 100 RP -18 (5 µm) was from Merck (Darmstadt, Germany). All other reagents were of the highest purity grade commercially available.

2.2. Animals

All procedures were performed in 6 month old male mice. Two groups were compared, wild-type mice from FVB/N strain (n=13, representing the control) and YAC128 transgenic mice with FVB/N background (n=12), both obtained from our local colony with breeding couples gently provided by Michael Hayden (University of British Columbia, Vancouver, Canada).

All animal studies were performed according to the Helsinki Declaration and EU guidelines (86/609/EEC). All mice were reared in cages, housed at CNC animal facilities, in controlled temperature and humidity room and maintained at 12 h light/dark cycle, with *ad libitum* access to water and food. At the end of the study, mice were sacrificed after anesthesia with Avertin® to collect tissues and blood, Blood was collected by intracardiacal punction with a heparinized syringe, and centrifuged at 5 000 *xg*, for 2 min, at 4º C, in an Eppendorf Centrifuge 5415C. The hematocrit-containing pellet was removed and serum was sampled into sterile eppendorf tubes and frozen at -20ºC to posterior analysis. Mice were perfused with PBS (1%) at PH 7.4 (0.2 M sodium phosphate dibasic, 0.2 M potassium phosphate monobasic) to eliminate blood clots from tissues and the brain was removed and dissected. One hemibrain was fixed in 4% paraformaldehyde, prepared in 0.1M PBS, pH 7.4. After the brain was settled, the solution was replaced by 20% glucose in PBS (1x), containing (~1%) sodium azide (a bacteriostatic compound that prevents bacterial contamination).

The other hemibrain was snap frozen at -80ºC for posterior analysis. Then, the hemibrain was unfrozen and homogenized in 2 ml PBS with a Potter-Elvejhem homogenizer with a Teflon pestle, at 300 rpm to obtain an homogenized, and kept at -20ºC.

2.2.1. Assessment of body weight and temperature

Body weight and temperature was assessed in early afternoon, before behaviour tests or glucose and insulin tolerance tests (GTT and ITT, respectively). Rectal temperature was monitored with a digital thermistor thermometer (Artsana®).

2.3. Genotyping

Three weeks old mice were genotyped by using a tail-tip DNA Polymerase Chain Reaction (PCR) procedure. PCR is a highly sensitive and specific technique for the amplification of nucleic acid (Kary Mullis, 1983). DNA was extracted from a portion of dissected mouse tail placed in an eppendorf tube containing proteinase K, by adding 700 µl of Lysis Buffer, according to a previously

described procedure (Mangiarini *et al*., 1999). The site of cleavage for this enzyme is the peptide bond adjacent to the carboxyl group of aliphatic and aromatic amino acids with blocked alpha amino groups (Manak, 1993). The main task consisted in protein digestion and removal of contaminants from preparations of nucleic acids, since they rapidly inactivate nucleases that may otherwise degrade DNA or RNA during purification (Manak, 1993). Preparations were incubated overnight at 56ºC. After this procedure, supernatant was removed and 200 µl of overconcentrated NaCl were added to each eppendorf tube. After a 2 min centrifugation at 14000 rpm, the pellet was removed and 500 µl of iced pure alcohol was added, forming a "cloud" of DNA. This "cloud" was removed and 700 µl of 70% alcohol was added to rehydrate. The supernatant was removed and the DNA attached to eppendorf tube was left to dry. DNA was resuspended with 200 µl of TE (Tris EDTA) and the optical density was spectrophotometrically measured at 260 nm and 280 nm, being the difference the value of interest which corresponds to the difference between the reference and a sample.

To perform PCR, Master Mix (containing buffer (5x), $MgCl_2$ (25 mM), dNTP (10 mM), primers and *Taq* polymerase) and milliQ water were added to the DNA sample, in a final volume of 25 µl, according to the procedure described by The Jackson Laboratories protocol. The primers were (Invitrogen®):

LyA1 – CCT GCT CGC TTC GCT ACT TGG AGC
LyA2 – GTC TTG CGC CTT AAA CCA ACT TGG
RyA1 – CTT GAG ATC GGG CGT TCG ACT CGC
RyA2 – CCG CAC CTG TGG CGC CGG TGA TGC
Actin Foward – GGA GAC GGG GTC ACC CAC AC
Actin Reverse – AGC CTC AGG GCA TCG GAA CC.

The PCR protocol consisted of 35 cycles with the following temperatures and times for each steps: denaturation – 94ºC for 30 s; annealing – 63ºC for 30 s; elongation – 72ºC for 30 s. At the end of the cycles, DNA was left at 70ºC for 10 min.

A 1,7% agarosis gel was made and the samples were mixed with DNA Loading Dye and pippetted onto the wells. Template was a DNA ladder with 100 bp. An agarosis gel electrophoresis was performed at a constant voltage of 120 mV. Gel imaging was acquired in a VersaDoc Imaging System® (BioRad, Hercules, USA), using BioRad Quantity One software.

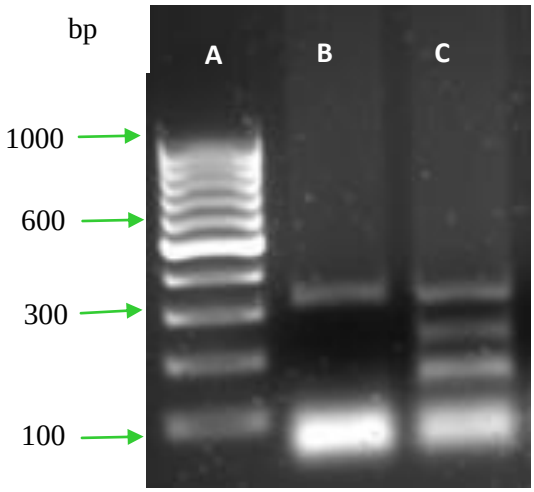

Fig. 2.1. PCR analysis of DNA extracted from mouse tail samples. Agarose gel analysis show distinct bands between 100-1000 bp after ethidium bromide staining (Fig. 2.1. A). Analysis of the PCR products on agarose gel allows a clear distinction between normal (Fig. 2. 1. B) and expanded alleles (Fig. 2.1. C). Lane A-Marker, Lane B – Wild-type mouse, Lane C – YAC128

2.4. Behaviour analysis

To measure motor ability, exploratory capacity and anxiety in mice, two behavioural test paradigms were performed: the rotarod and the open-field tests. Animals were brought in their cages to the test room at least 1 hr prior to the start of behavioural testing, where they remained until the beginning of the test. Procedures were consistent for all subjects, with tests made in lit room, temperature of 25^{o}C and minimum noise levels.

Behavioural equipment was cleaned thoroughly with 70% ethanol before and after each test session. After each animal completed its session, the equipment was also cleaned with 30% ethanol. In openfield test, the fecal *boli* and urine were removed and surfaces wiped out carefully, allowing the chamber to dry completely before another animal started the test. The experimenter wore a green lab coat during all the procedure.

2.4.1. Rotarod Test

The rotarod was designed to assess motor coordination, balance and equilibrium (Jones et al, 1968). The equipment (PanLab®) available in our laboratory allows the simultaneous assessment of 5 mice; however it was not the case in this study since we performed the tests individually. The rotarod unit has a base of *Perspex* with dimensions of 362 (wide) x 240 (diameter) x 400 (high) mm, an integrated drum (250 mm diameter) composed by a rod (30 mm diameter) and 5 lines (50 mm wide). Mice were gently grabbed by the tail and placed on the roller lane of the rotarod. Before the test,

performed as described by Carter *et al.*, (2001), mice were trained for 40 s at a constant speed of 4 rpm, to allow familiarization with the equipment. After a two hour, each mouse performed was tested for four sessions on the rod, with a gradual acceleration rate from 4-40 rpm during 5 min, each one separated by a 30 min resting period. When the animal fell off the rod, the time latency to fall and rotation speed were automatically recorded. Other mouse behavioural parameters (*e.g.* number of turns on the rod) were also registered. Results were expressed as latency to fall of rotarod (s).

2.4.2. Open Field Exploration Test

This test allows the assessment of novel environment exploration, general locomotor activity and an initial screen for anxiety-related behaviour (Gould *et al*., 2009). A session with an extended length (30 min) also provides reliable information about habituation to the increasingly familiar chamber environment (Bailey and Crawley, 2009. The system is composed by 2 square frames with 22 x 22 cm size, a frame support and a control unit. Chamber walls and floor are made of transparent Plexiglass. The open field arena is divided into a grid of equally sized areas by infrared photocell beams or lines drawn on the chamber floor, for visual scoring of activity by the experimenter. FRAMES (photo beam sensors) are equipped with 32 infrared photocells, 16 placed in axis X and 16 placed in axis Y. The photocell works at a wavelength of 950 nm and its information is multiplexed at a rate of 40Hz. The system gives data about fast (5 cm/s) and slow (2 cm/s) movements, fast and slow stereotypies, number of fast and slow rearing and number of fast and slow nose-pokes in the hole-board test.

Mice were tested for 30 min, as described by Gould *et al.* (2009) the room had lights on and a record was made with a digital camera. To start the test, the mouse was placed in the centre of the chamber. The experimenter left the testing rooms after this procedure, since sudden motion or noise could greatly affect exploratory activity. Mice were allowed to freely explore the chamber for 30 min and each line crossed or photocell beam break were scored as one unit of activity. Defecation and grooming activity were also scored. At the end of the test, the mouse returned to home cage. Results were expressed as mean±SEM.

2.5. Measurement of blood glucose levels

Blood was collected from the caudal vein and blood glucose levels were measured using a glucometer (The OneTouch® Ultra®,) with compatible stripes, based on the reaction of glucose oxidation to gluconolactone, catalyzed by glucose oxidase (Yoo and Lee, 2010). Under normal,

healthy conditions mouse glycemia after a 4 hour fasting is ~100 mg glucose/dl blood (between 60-130 mg glucose/dl blood) (Wong *et al.*, 1999). Immediately after a meal and before insulin has time to be released and remove glucose from blood into the cells, glycemia may increase, returning to ~100 mg/dl afterwards (Wong *et al.*, 1999). Results were expressed as mg glucose/dl blood.

2.6. Glucose Tolerance Test

Glucose tolerance test (GTT) analyses the rate of glucose clearance from blood (American Diabetes Association, 2009). Food was removed at about midnight and mice were kept fasted for 12 h, being GTT test performed around midday. Basal glycemia was measured before *D*-glucose injection, corresponding to time 0. Then, an intraperitoneal injection of 2 mg *D*-glucose/g body weight was given and glycemia were determined after 15, 30, 60 and 120 min. The injection was given after mouse immobilization by the back of the neck and then turned, with abdomen facing the experimenter. The tail was pull tightly back to avoid leg movement. Syringe needle containing the appropriate amount of glucose was inserted into the peritoneal cavity about 1cm inside of the mouse's right thigh, at a shallow angle. At the end of the test, cages were supplied with wet food. Results were expressed as mg glucose/dl blood.

2.7. Insulin Tolerance Test

Insulin tolerance test (ITT) analyses the capacity of cell membrane glucose transporters (GLUT) to uptake glucose, as a response to an increase in plasma insulin (Bruning, 1997).

Mice were kept fasted for two hours, from noon to 2 p.m., in their cages. Basal glycemia was measured before insulin injection, corresponding to time 0. Then, an intraperitoneal injection of 1µU human recombinant insulin/g body weight was given to mice and glycemia were determined at 15, 30, 60 and 120 min. At the end of the test, cages were supplied with wet food. Results were expressed as mg glucose/dl blood and as areas under the curve (AUCs), which were calculated using trapezoidal integration (Zou, 2001). Trapezoidal rule is a numerical integration method used to approximate the integral or the area under a curve. The integration of **[a, b]** from a functional form is divided into n equal pieces, called a trapezoid - $\int_a^b f(x)dx$. Each subinterval is approximated by the integrand of a constant value. In the case of GTT and ITT the integration was with the follow function: $\boldsymbol{AUC} = \left[\left(\frac{\mathbf{A}+\mathbf{B}}{\mathbf{2}}\right) * (\mathbf{C} - \mathbf{D})\right]$

Where:

A- Glucose levels time t_n

B- Glucose levels time t_{n-1}

C- t_n

D- t_{n-1}

2.8. Assessment of plasma and brain levels of Insulin

Plasma and brain insulin levels were measured with a two site enzyme immunoassay (ELISA - Enzyme Linked Immuno Sorbent Assay) from ALPCO. Briefly, this assay is based on the ability of an antibody to bind with high specificity to one molecule, called an antigen (Beatty *et al*., 1987). Importantly, this immunoassay produces a measurable signal in response to a specific binding (in this case by differences in light observation measured with a spectrophotometer). Herewith, a mouse monoclonal antibody specific for insulin is immobilized into a 96-well microplate as the solid phase. Standards, controls, and samples added to the appropriate wells with a horseradish peroxidase enzyme labelled monoclonal antibody (Conjugate) result in insulin molecules sandwiching between the solid phase and the Conjugate (ALPCO protocol).

According to manufacturer's instructions, brain homogenates and serum samples (10 µl) obtained as previously described were pippeted into the respective wells. Standards and reconstituted control were also placed in wells. Then, 75 µl of Working Strength Conjugate were pipetted into the wells and shaken for 2 h at 700-900 rpm, on a horizontal microplate shaker at room temperature. After incubation, the wells were washed with Wash Buffer to remove unbound Conjugate. Then, 100 µl of TMB Substrate were added to each well, and the microplate was incubated on a microplate shaker at room temperature for 15 min. During this incubation, a blue color results from TMB Substrate reacting with bound Conjugate in the wells. Reaction was stopped by adding 100 µl of Stop Solution and the colour changed from blue to yellow. Optical density was measured by microplate reader (SPECTRAmax PLUS®) at 450 nm, with a reference wavelength of 620 nm. The intensity of yellow color is directly proportional to the amount of insulin in sample. Results were expressed as mean ±SEM.

2.9. Assessment of plasma and brain levels of IGF-1

Brain and serum determination of insulin-like growth factor-I (IGF-I) levels was made using a Quantikine Mouse/Rat IGF-I Immunoassay from R&D Systems composed of a solid-phase ELISA

with *E. coli*-expressed recombinant mouse IGF-I and antibodies raised against the recombinant factor (Beatty *et al*., 1987). This assay employs the quantitative sandwich enzyme immunoassay technique, in which a monoclonal antibody specific for mouse/rat IGF-I has been pre-coated onto a microplate.

According to manufacturer's instructions, blood sera were diluted 500 times with Calibrator Diluent RD5-38, by adding 10 µl sample to 490 µl of Calibrator Diluent RD5-38. The 500–fold dilution was completed adding 15 µl of this solution to 135 µl of Calibrator Diluent RD5-38. Brain homogenates were diluted 6 times into Calibrator Diluent RD5-38, by adding 10 µl of homogenate to 50 µl of Calibrator Diluent RD5-38. Then, 50 µl of Calibrator Diluent RD5-38 was added to each well, followed by pippetting of 50 µl of standards, control, and samples into the same wells, allowing any mouse or rat IGF-I present to be bound by the immobilized antibody. After a 2 h incubation at room temperature on a horizontal orbital microplate shaker (GFL Shaker 3005®) at 500 ± 50 rpm, solution was removed from each well and washed with Wash Buffer to remove any unbound compounds. Then, 100 µl of Conjugated containing enzyme-linked polyclonal antibody specific for mouse/rat IGF-I was added to the wells and incubated for 2 h. Wells were washed again to remove any unbound antibody-enzyme reagent and 100 µl of a substrate solution were added to the wells, followed by a 30 min incubation under light protection. After the addition of 100 µl of Stop Solution, the enzymatic reaction-induced blue colour turned into yellow. The intensity of the colour measured is proportional to the amount of mouse or rat IGF-I bound in the initial step. Optical density of each well was measured using a microplate reader (GFL Shaker 3005®) at 450 nm, with a correction set to 540 nm. Sample values were then compared with those from standard curve. Results were expressed as mean ±SEM.

2.8. Assessment of brain levels of pyruvate and lactate

2.8.1. Pyruvate

In this colorimetric assay (Lactate Assay Kit from Abcam), oxidation of pyruvate by pyruvate oxidase generates colour (yellow) and its intensity is proportional to pyruvate levels (Sedewitz *et al*., 1984). Following manufacturer's instructions, reagents were prepared upon dilution of Pyruvate Probe with 220 µl of DMSO (Dimethylsulfoxide) and Pyruvate Enzyme Mix with 220 µl Pyruvate Assay Buffer. A Standard Curve was prepared by diluting Pyruvate Standard to a 1 nmol/µl concentration (10 µl of the Standard in 990 µl of Pyruvate Assay Buffer). Then, 0, 2, 4, 6, 8, 10 µl of this diluted Pyruvate Standard were added into each well and the final volume was adjusted to 50

µl/well with Pyruvate Assay Buffer to generate 0, 2, 4, 6, 8, 10 nmol of Pyruvate Standard. Pyruvate levels were measured in brain homogenates diluted in 4 volumes of Pyruvate Assay Buffer, and centrifuged to get a clear pyruvate extract. Sample volume was adjusted to 50 µl/well with Pyruvate Assay Buffer. Then, Reaction Mix containing the following components was prepared: 46 µl Pyruvate Assay Buffer; 2 µl Pyruvate Probe; 2 µl Enzyme Mix; and 50 µl of this preparation added to each well and incubated for 30 min at room temperature, protected from light. Optical density was measured at 570 nm. Results were expressed as mean±SEM.

2.8.2. Lactate

In the Lactate Assay Kit, lactate is oxidized by lactate dehydrogenase to generate a product that interacts with a probe to produce a colour (yellow), which can be detected spectrophotometrically at 450 nm. Reagents were prepared according to manufacturer's instructions by dissolving Lactate Enzyme Mix in 0,22 ml Lactate Assay Buffer, and Lactate Substrate Mix in 0,22 ml of Lactate Assay Buffer. A Standard Curve was prepared upon reconstitution of the Lactate Standard into a 1 mM stock solution (10 µl of the Lactate Standard to 990 µl of Lactate Assay Buffer). Then, 0, 1, 2, 3, 4, 5 µl were added to each well. Volumes were adjusted to 25 µl/well with Lactate Assay Buffer, to generate 0, 2, 4, 6, 8, 10 nmol of the L(+)-Lactate Standard. Lactate levels were determined in brain homogenates diluted with Lactate Assay Buffer, in a proportion of 10 µl of sample to 15 µl of buffer, and added to each well. Then, 25 µl of Reaction Mix (containing 23 µl Lactate Assay Buffer, 1 µl Lactate Substrate Mix and 1 µl Lactate Enzyme Mix) were prepared and added to each well and incubated for 30 min at room temperature, protected from light. Optical density was measured at 450nm in a microplate reader (GFL Shaker 3005®). Results were expressed as mean±SEM.

2.9. Analysis of Adenine Nucleotides and its Metabolites

Intracellular adenine nucleotides ATP, ADP, AMP were determined from brain homogenates, prepared as previously described. These samples were assayed by separation in a reverse-phase high-performance liquid chromatography, upon an isocratic elution with 100 mM phosphate buffer (KH2PO4), pH 6.5, and 1% methanol, with a flow rate of 1 ml/min, using a Lichrospher 100 RP-18 (5 µm) column, as described by Stocchi *et al*. (1985) The chromatographic apparatus used was a Beckham-System Gold, consisting of a 126 Binary Pump Model and 166 Variable UV detectors,

controlled by a computer. The detection wavelength was 254 nm and the time required for each analysis was 6 min. Peak identification was determined by following the retention time of standards.

Cellular energetic charge was calculated using the formula: ([ATP] + 0.5 [ADP])/([ATP] + [ADP] + [AMP]), as described by Pradet and Raymond (1983).

2.10. Data analysis and statistics

Results are the mean ±SEM of the indicated number of independent experiments, each corresponding to a single animal. Parametric tests were used such as *Student t* test for single comparison and one- or two-way ANOVA. A $P<0.05$ was considered significant.

PART II

RESULTS AND DISCUSSION

CHAPTER III

RESULTS

3.1. Analysis of diabetic parameters in YAC128 and WT mice

Initial experiments were focused on the analysis of total blood glucose levels in both heterozygous YAC128 mice and WT littermates, at 6 months of age. Data in Fig. 3.1 show similar (although relatively high) glycemia in both animals, under fasting or non-fasting conditions. A normal mouse should have blood glucose of around 100 mg/dl (ranging between 60-130 mg/dl) after 4 h fasting (Wong *et al*., 1999). Glycemia in WT and transgenic mice was higher than it should be expected from normoglycemic mice, namely 212.8 ± 14.71 mg glucose/dl blood for WT and 234.4 ± 16.72 mg glucose/dl blood for YAC128 mice under feeding conditions (Fig. 3.1A), and 132.8 ± 11.25 mg glucose/dl blood *versus* 133.0 ± 13.12 mg glucose/dl blood after 12 h fasting for WT and YAC128 mice, respectively (Fig. 3.1B). The observed hyperglycemia may be a symptom of diabetes mellitus in these animals. Thus, we further characterized YAC128 mice under a FBV/N strain with hyperglycemic background.

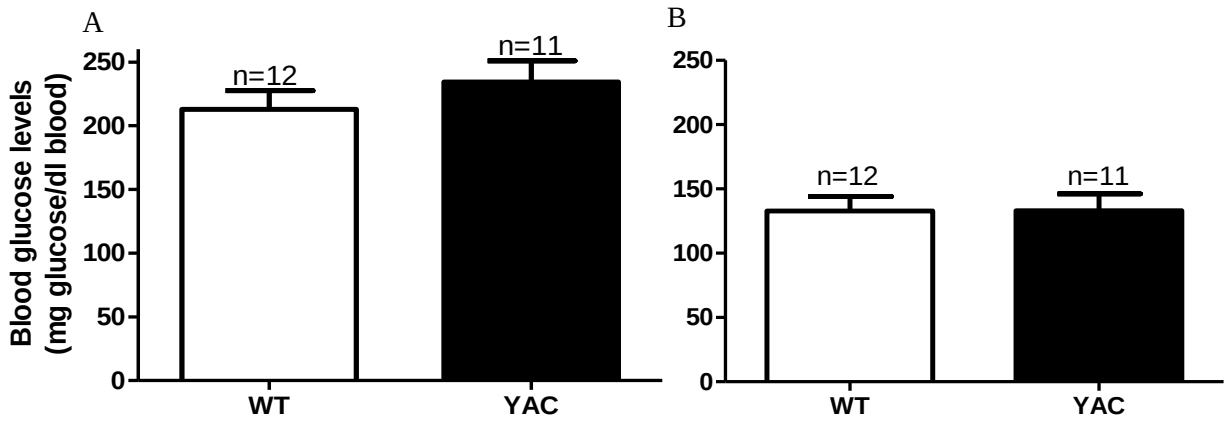

Fig. 3.1. Plasma glucose level in feeding conditions (A) and 12h fasting plasma glucose (B) in WT and YAC128 mice. Glucose levels, measured approximately at noon and after 12h fasting, show that both WT and YAC128 mice have a hyperglycemic background. The data are the mean±SEM of the indicated number of animals.

The glucose tolerance test measures the clearance of a standardized glucose load from the body (Andrikopoulos *et al*., 2008**)**. No significant changes in blood glucose levels were observed during the GTT in YAC128 or WT mice in response to the administration of high glucose levels (Fig. 3.2A). The area under the curve (AUC) showed a non-statistical variation of 6.5% between both genotypes (Fig. 3.2B). The values for the curves were 37310 ± 3038 mg/dl x h for WT and 39920 ± 4089 mg/dl x h for YAC128 mice.

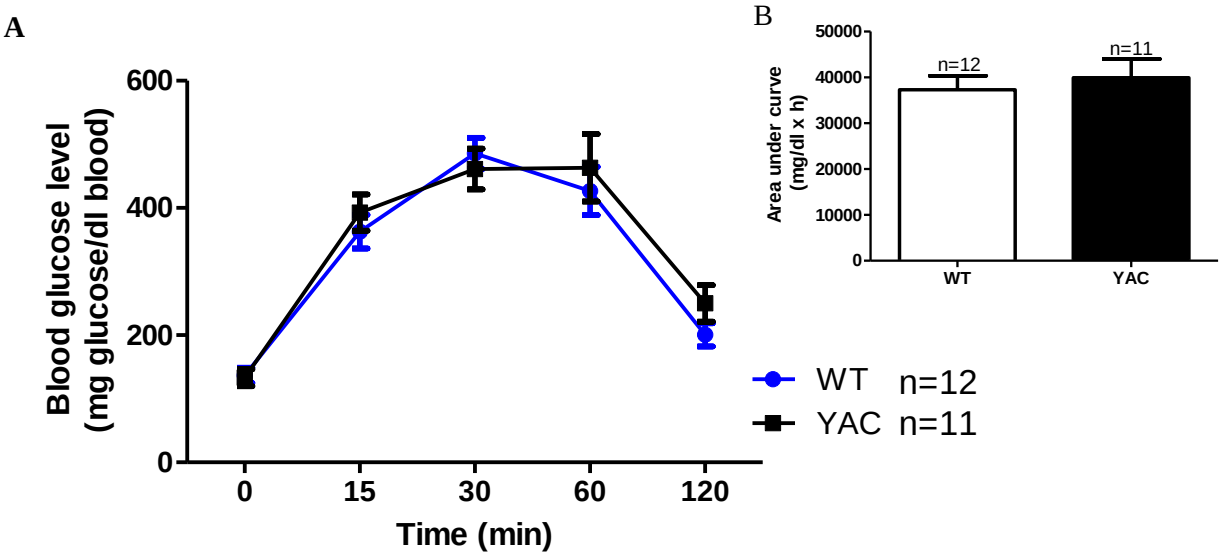

Fig. 3.2. Glucose Tolerance Test (A) and Area Under the Curve (B). Glucose (2 mg/g body weight) was intraperitoneally administered. Blood glucose levels were measured after 0, 15, 30, 60 and 120 min. AUC was calculated from data in Fig.3.2A. The data are the mean±SEM of the indicated number of animals.

Since no changes were found on the GTT, we also performed the Insulin Tolerance Test (ITT) to better characterize the diabetes in these animals and exploit insulin sensitivity/resistance. ITT measures the cells ability to use insulin after intraperitoneally administration, by measuring blood glucose levels at regular intervals (Carvalho *et al.*, 2005) (Fig. 3.3). YAC128 mice showed increased glycemia in response to insulin administration, as compared to WT mice. In YAC mice at 15 min, blood glucose levels raised significantly compared to WT mice (179.83 ±15.57 mg glucose/dl blood for WT *versus* 256.73 ± 19.21 mg glucose/dl blood for YAC128 mice, $p<0.01$) and then stabilized at 30-90 min. At 60 min, the difference between the two groups was again significant (146.92±12.46 mg glucose/dl blood for WT *versus* 212.09±15.23 mg glucose/dl blood for YAC128 mice, $p<0.05$). Interestingly, WT mice did not respond to insulin administration.

In agreement with the alterations found in ITT traces, the AUC for YAC 128 mice was 23.32 % higher than for WT mice ($p<0.05$). The mean ± SEM) values calculated for the AUCs were 14830 ± 1189 mg/dl x h for WT and 19340 ± 1236 mg/dl x h for YAC128 mice.

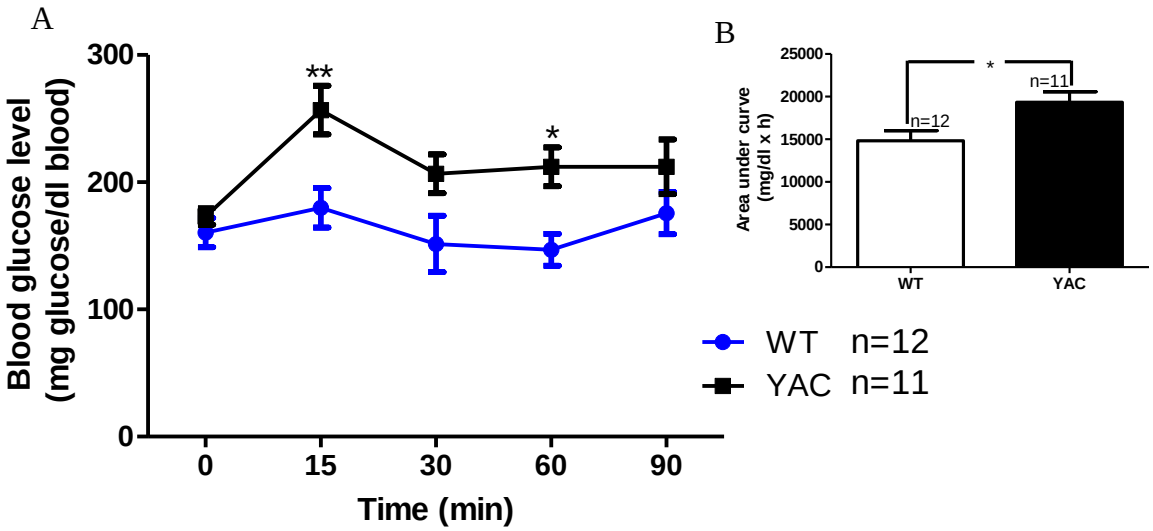

Fig.3.3. Insulin Tolerance Test (A) and Area Under Curve (B). Insulin (1 µU/g body weight) was intraperitoneally administered and serum glucose levels were measured after 0, 15, 30, 60 and 90 min. AUC was calculated from data in Fig.3.3A. Data are the mean±SEM of the indicated number of animals. Statistical significance: *p<0.05 or **p<0.01 *versus* WT mice.

Since insulin resistance appears to occur in controls, and a significant increase in total blood glucose levels were found in YAC128 in the ITT test, compared to WT mice, we further determined the plasma insulin levels in both groups of mice.

In YAC128 mice, we observed a tendency for lower plasma levels of insulin; however the values were not statistically significant (0.052 ± 0.008 ng/ml/mg protein for WT and 0.0331 ± 0.008 ng/ml/mg protein for YAC128 mice) (Fig. 3.4 B).

Because the neurotrophic factor IGF-1 has a primordial role on glucose metabolism (Petersson *et al*, 2009) and plasma IGF-1 may regulate body weight in HD (Pouladi *et al.*, 2010), we also determined plasma levels of IGF-1 in both WT and YAC128 mice under a minimum of 12 h fasting.

We observed a slight reduction, although not significant, in plasma IGF-1 levels in YAC128 (19.80 ± 1.00 ng/ml/mg protein), in comparison with WT (27.89 ± 3.92 ng/ml/mg protein) mice.

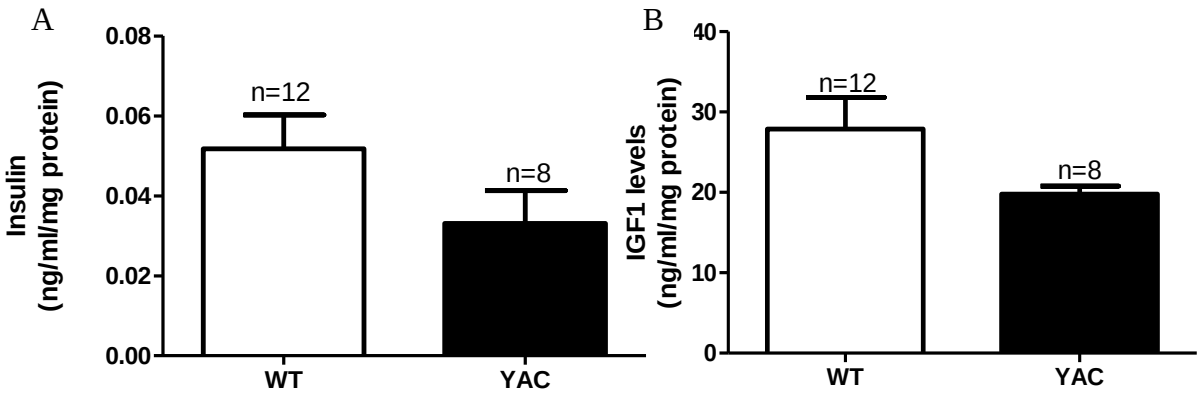

Fig. 3.4.Plasma Insulin (A) and IGF-1 (B) levels (A) in WT and YAC128 mice.
Data represent the mean±SEM of the indicated number of animals.

According to Pouladi *et al*. (2010) plasma IGF-1 levels are correlated with body weight in HD mice. Therefore, we measured mice body weight (Fig. 3.5.A) and temperature (Fig. 3.5.B). Both WT and YAC128 mice (6 months old), with the same FBV/N background, were overweighed; however, we did not find significant differences in body weight between YAC128 and WT mice.

The normal average rectal temperature for mice is 37.5^{o} C, varying during the day and with fasting conditions. Weydt *et al.* (2006) observed that N171-82Q HD mice develop hypothermia associated with impaired activation of brown adipose tissue. In our study, the temperature obtained was in the normal range for both groups and no statistical differences were found (36.46 ± 0.46^{o}C for WT and 36.86 ± 0.33^{o}C for YAC128 mice).

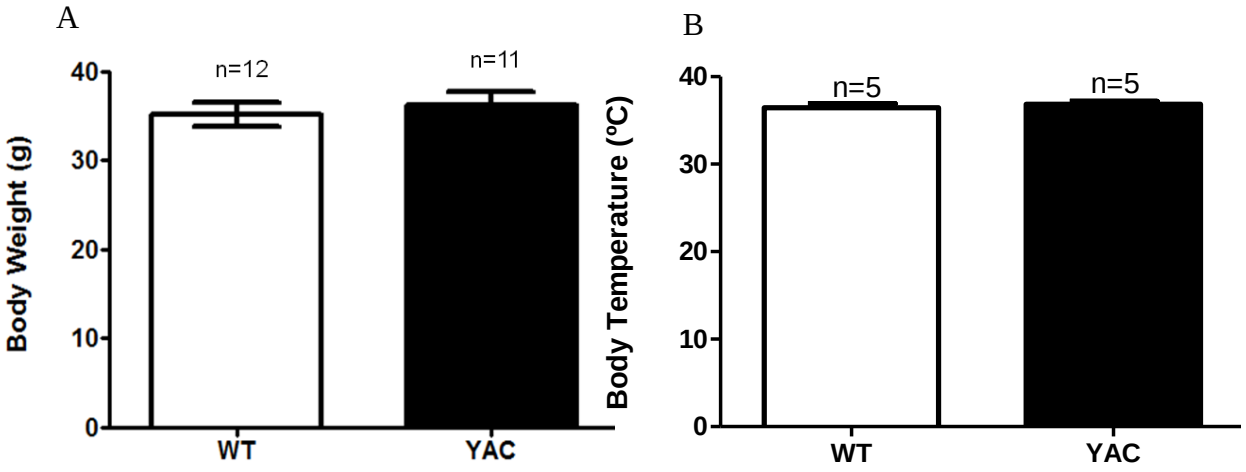

Fig. 3.5. Characterization of YAC128 and WT mice based on body weight (A) and temperature (B). When compared, the two groups are very similar, showing no statistical differences in body weight and body temperature. Data represent the mean±SEM of the indicated number of animals.

3.2. Behaviour analysis

YAC128 mice model of HD has been described to show motor impairment around 6 months of age (Slow *et al.*, 2003). Since the mice used in the present study showed an hyperglycemic background, we further analysed if it could influence/aggravate motor performance. Using an accelerating rotarod to examine fall latency, YAC128 mice showed a tendency (22.1%) for a decrease in latency to fall off the rotarod compared to WT mice, although it did not reach statistical significance (Fig. 3.6), suggesting a tendency for motor impairment.

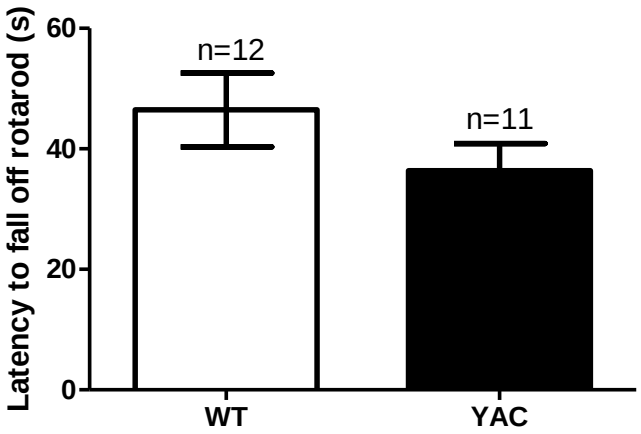

Fig. 3.6. Behaviour characterization of YAC128 versus WT mice by the rotarod test. YAC128 and WT mice littermates were tested in four trials on an accelerating rotarod at 6 months of age. Data represent the mean±SEM *of the indicated number of animals.*

Mouse locomotor activity was further measured using an open-field apparatus for a period of 30 min. YAC128 mice appeared to have similar locomotion and exploration behaviour profiles (Fig. 3.7). No statistical differences for WT *versus* YAC128 mice were found for maximal (14.47±0.53 cm/s *versus* 14.13 ±0.77 cm/s or mean velocity (1.60±0.21 cm/s *versus* 1.53±0.19 cm/s) (Fig. 3.7.A). The distance travelled (2921 ± 370.0 cm *versus*. 2750 ± 333.7 cm) (Fig. 3.7.B) and the resting time (63.65 ± 3.20 s *versus* 64.86 ± 3.24 s) were similar between WT and YAC128 mice (Fig. 3.7.C). Slow and fast movements did not show any significant differences between groups (Fig. 3.7.D). The values obtained for number of slow movements were 261.85 ±32.58 for WT *versus* 260.47±38.71 for YAC128 mice, and for number of fast movements were 392.73±31.25 for WT *versus* 371.89±22.68 for YAC128 mice. The latter showed a tendency for a decrease in the number of rearings (Fig. 3.7.F), which may be due to less anxiety during the test. The permanence time in central square was not different between controls and transgenic animals (55.90 ± 3.767% of total time *versus* 60.48 ± 3.766% of total time in WT and YAC128 mice, respectively) (Fig. 3.7.E).

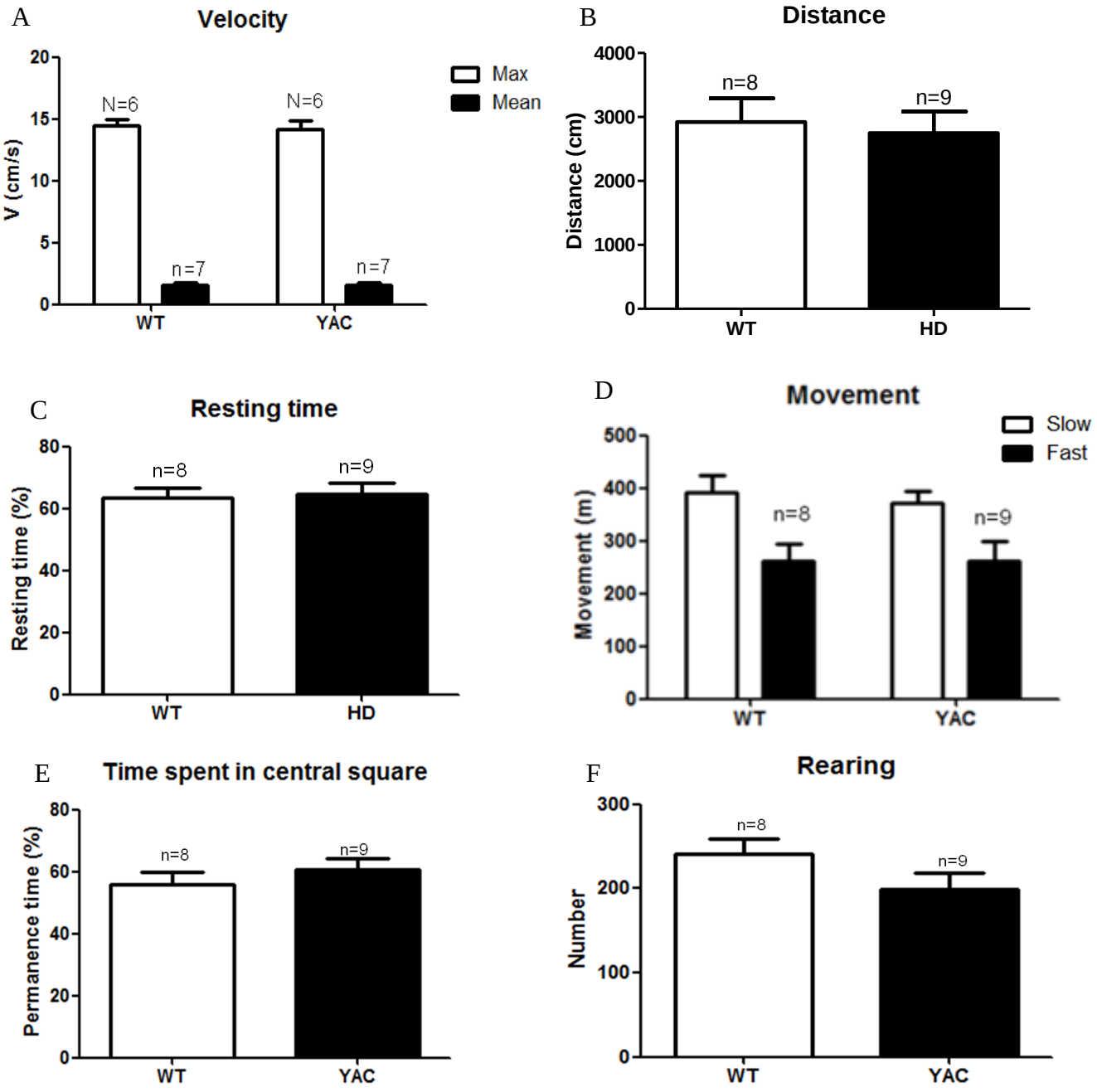

Fig. 3.7. Behaviour characterization of YAC128 versus WT mice by the openfield test. YAC128 and control (WT) littermates were tested in an openfield activity box over a period of 30 min. Six activity parameters were measured: A-mean and maximal velocity (cm/s); B-distance travelled (cm); C-resting time (s); D-slow and fast movements; E –Time spending in central square; F – Rearing.- Data represent the mean±SEM of the indicated number of animals.

Given the tendency for a deficit in motor performance in YAC128 mice, as evaluated by the rotarod test, which may be caused by neuronal dysfunction (Slow et al., 2003), we further analysed central metabolic parameters in order to contextualize those alterations.

HD is characterized by neuronal impairment, which causes early energy deficit in HD brain (Koroshetz *et al.*, 1997). Indeed, our results showed a significant reduction (by approximately 39%) in energy charge in YAC128 compared to WT mice (60.97 ± 6.227 % of WT values) (Fig. 3.8.).

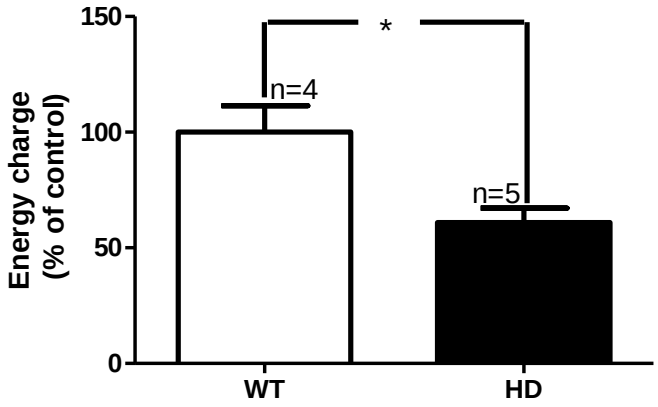

Fig. 3.8. Brain energetic charge in YAC128 and WT mice. Brain energetic charge was calculated as ([ATP] + 0.5 [ADP])/([ATP] + [ADP]+[AMP]). Data expressed as percentages of the ATP/ADP ratio in WT control mice brain (considering 0.77 ± 0.09 as 100%). Data are the mean±SEM of the indicated number of animals. Statistical significance: * $p<0.05$, as compared to WT mice.

Analysis of brain lactate and pyruvate are useful to screen for impaired energy metabolism. Elevated lactate may be suggestive of mitochondrial dysfunction, and is found in several neurodegenerative disorders, namely Alzheimer, Parkinson and HD (Bowling and Beal, 1995). Thus, lactate/pyruvate (L/P) ratio is a marker of cytoplasmatic redox status and glycolytic function (Broderick *et al*., 2005). These values are typically elevated in disorders of oxidative phosphorylation associated with glycolytic overactivation, including HD (Oláh *et al*., 2008). The normal L/P ratio should be <20:1 (Sattler *et al*., 2008).

Lactate levels in brain of WT and YAC128 mice did not differ significantly (6.82 ± 1.28 nm/µl/mg protein for WT and 5.49 ± 0.48 nm/µl/mg protein for YAC128 mice) (Fig. 3.9.A.). However, brain pyruvate levels were significantly decreased in YAC128 compared to control mice (3.56 ± 0.47 nm/µl/mg for WT *versus* 1.75 ± 0.39 nm/µl/mg for YAC128 mice, $p<0.05$) (Fig. 3.9.B).

L/P ratio calculated for both groups was in the normal range for mice brain (Sattler *et al*., 2008), but YAC128 mice showed a tendency for higher values than the controls (1.91 ± 0.22 for WT and 3.86 ± 1.12 for YAC128 mice) (Fig. 3.9.C).

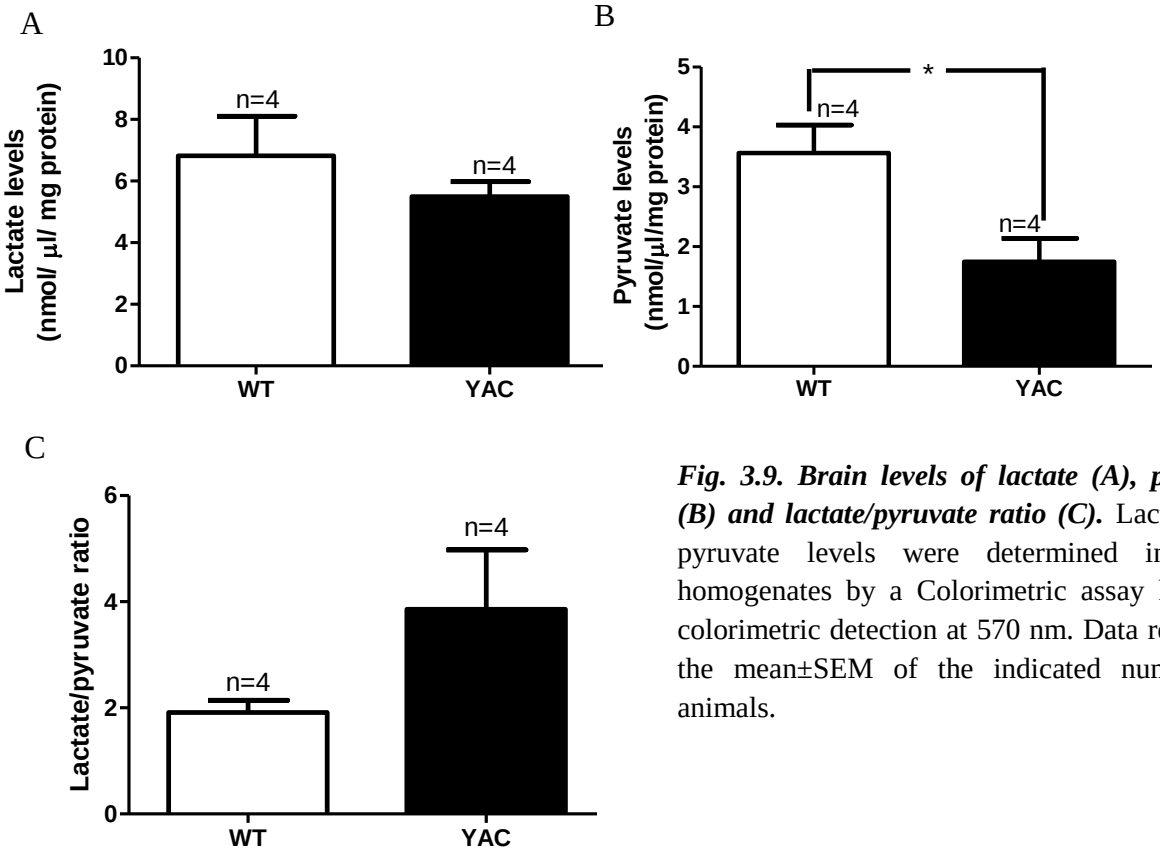

Fig. 3.9. Brain levels of lactate (A), pyruvate (B) and lactate/pyruvate ratio (C). Lactate and pyruvate levels were determined in brain homogenates by a Colorimetric assay kit with colorimetric detection at 570 nm. Data represent the mean±SEM of the indicated number of animals.

IGF-1 and insulin were also measured in total brain homogenates from YAC128 and control (WT) mice. Brain insulin and IGF-1 levels were not significantly different between WT and YAC128 mice (91.90±14.89 pg IGF-1/ml/mg protein for WT and 74.25±11.00 pg IGF-1/ml/mg protein for YAC128 mice; 04175±0.02330 ng insulin /ml/mg protein in WT and 0.03627±0.01378 ng insulin /ml/mg protein in YAC128 mice). (Fig. 3.10).

The brain data presented in Fig. 3.10. correspond to a reduced number of animals (n=3 to 5), compared to the number of animals used to determine plasma insulin and IGF-1 levels (n= 8 to 12) (Fig.3.10).

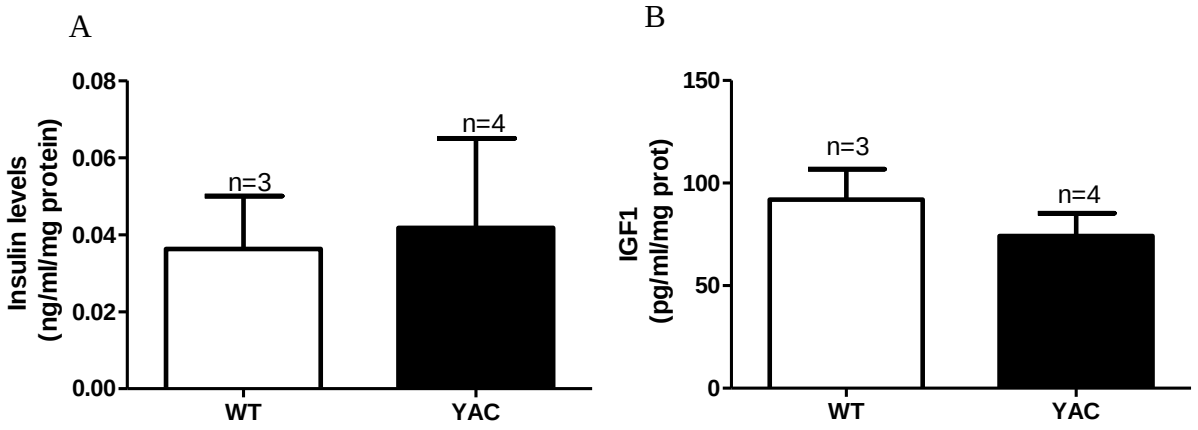

Fig. 3.10. Brain levels of insulin (A) and IGF-1 (B). Insulin levels were determined in brain homogenates by an ELISA kit with colorimetric detection at 450 nm, with a reference wavelength of 620 nm. Data represent the mean±SEM of the indicated number of animals.

CHAPTER IV

DISCUSSION

4. Discussion

YAC128 mice are well characterized in terms of neuronal loss and disease progression but, so far, only few studies have focused on peripheral and cerebral metabolism. This mouse strain presents several features of HD, namely motor impairment, cognitive deficits and neuronal loss in the striatum, an area that comprises a large number (90-95%) of GABAergic medium spiny neurons (Slow *et al.*, 2003; van Raamsdonk *et al*., 2007).

Interestingly, our study showed that both WT and YAC128 transgenic mice exhibit elevated glycemia, compatible with diabetes mellitus, either type 1 or 2, depending on the pathophysiology involved, insulin-dependent or -independent, respectively. The current World Health Organization diagnostic criteria for diabetes refers that blood glucose levels during fasting should be higher than 126 mg glucose/dl blood, or 200 mg glucose/dl blood for 2 h blood glucose (WHO, 1996). Indeed, in our study both groups had higher values, approximately 133 mg/dl for fasting glucose levels. HD has been associated with endocrine abnormalities, namely diabetes, glucose intolerance and insulin resistance, even in normoglycemic patients (Podolsky *et al.*, 1997; Ferrer, 1985; Lalić *et al.*, 2008). Ferrer (1985) found that 10.5% of HD patients developed diabetes, suggesting that this condition may be approximately 7 times more often in these patients than in matched control participants. These metabolic changes have been also reproduced in transgenic mice, such as the R6/2, R6/1 and N171-82Q mice (Schilling *et al*., 1999, Bjőrkqvist *et al,* 2005, Josefsen *et al.,* 2008), suggesting that diabetes could be a cardinal feature of HD progression. Bjőrkqvist *et al.* (2005) have previously reported that diabetes in R6/2 mice may be a consequence of pathogenic mechanisms occurring due to polyQ inclusions in pancreatic β-cells.

In our results, using the YAC128 mice, we found that the response to GTT was similar in both groups. However, we observed significant changes in the ITT, which could be related with insulin sensitivity. Indeed, WT mice did not respond to intraperitoneal injection of 1 μU human recombinant insulin/g body weight, whereas HD mice showed some sensitivity to insulin during the test, as blood glucose levels tend to decrease. This difference could reflect an insulin resistance in WT, since no changes in glucose levels were observed. This was not observed in transgenic mice, suggesting that this mechanism may not be responsible for diabetes in these animals. Another possible explanation for the poor response in ITT could be related with the dose of insulin used. Some studies used higher doses of insulin when performing the ITT in mice (Brüning *et al,*. 1997). Furthermore, others suggested that insulin resistance/insensitivity may not be the major reason for developing diabetes, but rather the decrease in insulin expression (Hunt *et al.*, 2005). Interestingly, in

the HD mice group we also observed a non significant decrease (by approximately 36%) in the amount of circulating insulin, compared to WT mice. Ubiquitinated polyQ inclusions may appear in all cells, including pancreatic β-cells, originating aggregates that were suggested to impair insulin secretion (Bjőrkqvist *et al.*, 2005). In this regard, a reduction in β-cell mass and in vesicles containing insulin were shown as the main causes of hyperglycemia in R6/2 mice expressing the exon-1 of human mHtt (corresponding to ~3% of the total protein) (Bjőrkqvist *et al.*, 2005). In HD patients some controversial data have been published. Recently, a study concluded that HD patients do not have an increased risk of developing diabetes (Boesgaard *et al.*, 2009); however, other studies refer a high prevalence of glucose impairment and insulin resistance in HD (for review, Lalić *et al.*, 2008).

Hyperglycemia observed in the mice used in our study may also reflect a high caloric diet, since normal weight for FBV/N mouse strain is between 25-30 g (Pouladi *et al*., 2010) and ours largely exceeded those values. Previous studies have clearly shown that, when submitted to high-fat diet, this strain develops insulin resistance and reduced stimulated insulin secretion (Junghyo et al., 2009), which may aggravate the hyperglycemia in our predisposing transgenic mice. It was previously described that transgenic mice expressing full-length human mHtt, such as BACHD and FVB-YAC128 mice, start to gain weight, compared to WT mice, after 2 months of age, which is related with the background strain in which they were developed (Van Raamsdonk *et al.*, 2007). The YAC128 mice were initially developed in FVB background, but due to several problems associated with the strain, a few years later they were backcrossed onto the 129 and C57BL/6 strain backgrounds. Both FVB/N and 129 mice are known to be more susceptible to excitotoxicity (Schauwecker *et al.*, 1997) than C57BL/6 strain (Leonard *et al.*, 2002). At 12 months of age, striatal volume loss was significant in all three strains, being most affected in the FBV strain (van Raamsdonk *et al.*, 2007). The severity of the disease phenotype appears to be modulated by the background, being the FVB-YAC128 mice the most affected, probably due to the earliest appearance of nuclear inclusions of mHtt that correlate with more severe striatal neuropathology (van Raamsdonk *et al.*, 2007). Comparing the three backgrounds, FVB, 129 and C57Bl/6 mice, the FVB-YAC128 mice were the only that presented an increase in body weight and reduced lifespan (van Raamsdonk *et al*, 2007).

Pouladi *et al.* (2010) have recently found a positive correlation between plasma levels of IGF-1, modulated by full-length Htt, and body weight in YAC128 mice. IGF-1 is an essential modulator of growth hormone action, acting as a neurotrophic and anabolic factor (for review, Juul, 2003). Our

results showed similar IGF-1 levels in WT and YAC128 mice, reflecting their similar body weight. In Pouladi's study, IGF-1 values were slightly higher in both groups compared to ours. Their plasma values varied between 260 and 300 ng IGF-1/ml plasma (being lower for WT mice), and ours were 226.1±19.6 ng IGF-1/ml plasma for WT and 234.4±32.9 ng IGF-1/ml plasma in YAC128 mice. In transgenic mice, plasma levels of IGF-1 and insulin were slightly decreased (although not significantly). A possible explanation for this involves the pathophysiology of diabetes, since it has been shown that IGF-1 levels decrease with diabetes duration and with increased blood glucose, suggesting that IGF-1 may also play a role in peripheral uptake of glucose (Clauson *et al*., 1998). Low circulating levels of IGF-1 after hepatic deregulation in diabetes may underlie not only neuropathies associated with diabetes, but also the association of diabetes with different neurodegenerative diseases, including HD and Alzheimer disease (Arvanitakis *et al*., 2004). Suppression of IGFBP-1 (IGF-1 binding protein) by insulin may increase bioavailability of IGF-1, which could lead to an higher inhibition of growth hormone release in the pituitary gland and a consequent reduction in the production of IGF-1 in the liver (Sandhu *et al.*, 2002). In transgenic models of hepatic IGF-1 gene deletion, low concentrations of total circulating IGF-1 were associated with impaired insulin signalling in skeletal muscle and insulin resistance (Juul, 2003). Moreover, diabetes mellitus was previously associated with a decrease in mRNA transcripts for IGF-1, resulting in a lower concentration of circulating IGF-1 and in the levels of mRNA for its receptors (Bitar *et al*., 1997). In contrast, high total levels of IGF-1 reduced the susceptibility to deterioration of pancreatic β-cell mass and function, two important determinants of development of glucose intolerance (Clauson, *et al*., 1998, Sandhu *et al*., 2002). Recently, a large cohort study showed that adults over 65 years with glucose intolerance had lower IGFBP-1 levels compared to those with normal glucose tolerance (Rajpathak *et al*., 2008).

At 6 months of age, our transgenic mice performed slightly worse in the rotarod behaviour test than their WT littermates, which is in agreement with the initial description by Slow *et al*., (2003). The phenotype of YAC128, which includes motor impairment, is most likely related to one of the hallmarks of HD onset in patients, the striatal atrophy associated with significant neuronal loss (Slow *et al*., 2003). In this model, a linear correlation between rotarod performance at 6 and 9 months and neuronal loss at 12 months of age was previously established (Slow *et al*., 2003). Moreover, the appearance of early nuclear inclusions of mHtt in striatum seems to precede selective degeneration in this brain area, later seen in the disease (van Raamsdonk *et al*., 2007).

In brain, no significant differences in insulin or IGF-1 levels were observed in YAC128 mice compared to WT controls, although IGF-1 levels show a tendency to reduction in YAC128 mice. To better clarify this trend, a higher number of animals should be further tested. IGF-1 is one of the most important activators of Akt signaling pathway, a stimulator of cell growth and proliferation, and a potent inhibitor of apoptosis processes (for review, Trejo *et al*., 2004). Changes in IGF-1 levels were seen in some neurodegenerative disorders, like HD and Parkinson disease and based on its biological activities, it is reasonable to assume that IGF-1 depletion may contribute to the progress of neurodegenerative processes (for review, Trejo *et al*., 2004). In HD there is clear evidence that IGF-1/Akt neuroprotective pathway is altered (Humbert *et al*., 2002, Colin *et al*., 2005). A recent study found that IGF-1 mRNA expression and protein levels in striatal tissue of YAC18 mice were significantly higher than in WT control mice (Pouladi *et al*., 2010). Since our results were determined in total brain, it becomes difficult to confirm the striatal changes.

The main Gibbs energy source in brain is glucose, which is metabolized in the cytosol, via glycolysis, to generate pyruvate, from which the terminal oxidation machinery in the mitochondrial compartment produces the major amounts of ATP in neurons (Oláh *et al*, 2008). It has been widely shown that this process is deficient in neurodegenerative diseases and lactate/pyruvate ratio is typically elevated, due to increased regional brain lactate production (Martin *et al*. 2007). Our results are in agreement with the results obtained by other studies (Martin *et al*, 2007; Oláh *et al*, 2008), since YAC128 mice showed a higher lactate/pyruvate compared to WT littermates. Nevertheless, mHtt is known to interact with enzymes fundamental to the development of glycolysis, namely GAPDH (glyceraldehyde-3-phosphate dehydrogenase), partially inhibiting its function (Junchao *et al*., 2007). It is also widely recognized the relationship between mHtt and mitochondrial dysfunction, namely by interfering with oxidative phosphorylation (Bossy-Wetzel *et al*., 2008). This interaction occurs mainly with proteins of the respiratory chain, reducing their activity and compromising energy metabolism (Milakovic *et al*., 2005). MHtt also induces transcriptional dysregulation that may contribute to the mitochondrial dysfunction in HD. Studies with PGC-1α (peroxisome proliferator-activated receptor gamma coactivator 1-alpha) showed reduced levels in MSN due to mHtt-mediated transcriptional blockage, resulting in HD-linked mitochondrial deficits (Cui *et al*., 2006; Bossy-Wetzel *et al*., 2008). PGC-1α is a key transcriptional co-regulator and induces the transcription of cellular programs regulating mitochondrial respiration, oxidative stress defense and adaptive thermogenesis (Puigserver *et al*., 2003). Brain lactate content is increased in our transgenic model, resembling changes found in HD patients (Martin *et al*., 2007). Bioenergetic abnormalities

were also observed in our study through the reduction in energy charge in YAC128 mice brain. This energetic deficit in neurons may worse with neuronal loss and disease progression and may aggravate the symptoms of the disease.

In conclusion, we identified metabolic changes either in WT and YAC128 mice with a FBV background. Both have an hyperglycemic background that may influence the results obtained. Further studies with a large number of animals will certainly provide a better clarification of the influence of an hyperglycemic background in the phenotype and metabolism in this experimental model of HD. The data herein presented highly suggest that expression of full-length mHtt in YAC128 mice induces both peripheral and central metabolic changes potentially associated with decreased plasma insulin levels and deficient brain energy metabolism, which correlate with motor impairment. In this perspective, this study may highlight the role of full-length mHtt in the susceptibility of HD patients to undergo metabolic deregulation and diabetes.

List of Abbreviations

3-NP, 3-nitropropionic acid

Aa, amino acids

ADP, adenosine diphosphate

Akt, protein kinase B

AMP, adenosine monophosphate

AMPA, 3-hydroxy-5-methyl-4-propionate

Ask1, apoptosis signal-regulating kinase 1

ATP, adenosine triphosphate

AUC, area under the curve

BDNF, brain-derived neurotrophic factor

CAG, cytosine-adenine-guanine

cAMP, cyclic-adenosine monophosphate

CGG, cytosine-adenine-guanine

CNS, central nervous system

CREB - cyclic-adenosine monophosphate response element binding protein

CTG, cytosine- thymine-guanine

D1, subtype 1 dopamine receptor

D2, subtype 2 dopamine receptor

DA, dopamine

EGF, Epidermal growth factor

ELISA- Enzyme Linked Immuno Sorbent Assay

EMG, electromyography

ER, endoplasmic reticulum

GAA, guanine–adenine-adenine

GABA, γ–aminobutyric acid

GAD, glutamic acid decarboxylase

GAPDH, glyceraldehyde-3-phosphate dehydrogenase

GCC, guanine-cytosine-cytosine

GLUT, glucose transporter

GPe, external segment of the *globus pallidus*

GPi, internal segment of the *globus pallidus*

GTT, Glucose Tolerance Test

HAP1, Huntingtin associated protein 1

HD, Huntington's disease

HIP1, huntingtin-interacting protein 1

HIP2, huntingtin-interacting protein 2

HIPPI, HIP1-protein interactor

HSPs, Heat shock proteins

Htt, huntingtin

Htt^{NT}, N-terminal fragments

IGF-1, insulin growth factor 1

InsP3R1, inositol 1,4,5-trisphosphate receptors

IP31, inositol (1,4,5)-trisphosphate type 1

IT15, *Interesting Transcript 15* gene

ITT, Insulin Tolerance Test

KA, Kainic acid

L/P ratio, lactate/pyruvate ratio

MA, malonic acid

mGluR, metabotropic glutamate receptors

mHtt, mutant huntingtin

mPTP, mitochondrial permeability transition pore

MSN, medium spiny neurons

NAD^+, nicotinamide-adenine dinucleotide

NMDAR, *N*-methyl-D-aspartate receptor

NR2, NMDA receptor subunit

NTL, *nucleus tuberalis lateralis*

PBS, phosphate buffered saline

PCR, polymerase chain reaction

PGC-1α, peroxisome proliferator-activated receptor gamma coactivator 1-alpha

polyQ, polyglutamine(s)

QA, Quinolinic acid

REST, repressor element-1 transcription factor

ROS, reactive oxygen species

SBMA, Spinal and Bulbar Muscular Atrophy

SDH, succinate dehydrogenase

SNARE, ethylmaleimide-sensitive fusion protein attachment protein receptor

SNpc, *substantia nigra pars compacta*

SNr, *substantia nigra pars reticulata*

SP1, specific protein-1

STN, subthalamic nucleus

TAF_{II}, TATA-associated factors

TBP, TATA-binding protein

UPS, ubiquitin–proteasome system

UPS, ubiquitin–proteasome system

VA/VL complex, ventral anterior and ventral lateral thalamic nuclei

WHO, World Health Organization

YAC, yeast artificial chromosome

YAC, yeast artificial chromosome

References

Alders J, Smits M, Kremer B, Naarding P. The Role of Melatonin in Sleep Disturbances in End-Stage Huntington's Disease. J Neuropsychiatry Clin Neurosci. 2009;21(2):226-7.

American Diabetes Association. Standards of medical care in diabetes. Diabetes Care. 2009;32:S13-S61.

Andreassen OA, Dedeoglu A, Stanojevic V, Hughes DB, Browne SE, Leech CA, Ferrante RJ, Habener JF, Beal MF, Thomas MK. Huntington's disease of the endocrine pancreas: insulin deficiency and diabetes mellitus due to impaired insulin gene expression Neurobiol Dis. 2002;11(3):410-24.

Andrikopoulos S, Blair AR, Deluca N, Fam BC, Proietto J. Evaluating the glucose tolerance test in mice. Am J Physiol Endocrinol Metab. 2008;295(6): 1323-1332.

Arning, L., Kraus, P.H., Valentin, S., Saft, C., Andrich, J., Epplen, J.T.NR2A and NR2B receptor gene variations modify age at onset in Huntington disease. Neurogenetics 2005; 6:25–28.

Arvanitakis Z, Wilson RS, Bienias JL, Evans DA, Bennett DA. Diabetes mellitus and risk of Alzheimer disease and decline in cognitive function. Arch Neurol. 2004;61(5):661-6.

Ashwani K. Thakur, Murali Jayaraman, Rakesh Mishra, Monika Thakur, Veronique M. Chellgren, In-Ja Byeon1, Dalaver H. Anjum1, Ravindra Kodali1,2, Trevor P. Creamer3, James F. Conway1, Angela M.Gronenborn1, and Ronald Wetzel. Polyglutamine disruption of the huntingtin exon1 N-terminus triggers a complex aggregation mechanism. Nat Struct Mol Biol. 2009; 16(4): 380–389.

Aylward EH, Li Q, Stine OC, Ranen N, Sherr M, Barta PE, Bylsma FW, Pearlson GD, Ross CA. Longitudinal change in basal ganglia volume in patients with Huntington's disease. Neurology. 1997;48(2):394-9.

Bailey K, Crawley J. Methods of Behavior Analysis in Neuroscience, 2nd ed. Augusta, Boca Raton (FL): CRC Press; 2009.

Bates G. The molecular genetics of Huntington disease — a history. Nature 2005, 6:766-773.

Beatty, J.D., Beatty, B.G., and Vlahos, W.G. Measurement of monoclonal affinity by noncompetitive immunoassay. J. Immunol. Methods, 1987; 100:173-179.

Bennett EJ, Shaler TA, Woodman B, Ryu KY, Zaitseva TS, Becker CH, Bates GP, Schulman H, Kopito RR. Global changes to the ubiquitin system in Huntington's disease. Nature. 2007; 448(7154):704-8.

Bhide PG, Day M, Sapp E, Schwarz C, Sheth A, Kim J, Young AB, Penney J, Golden J, Aronin N, DiFiglia M. Expression of normal and m huntingtin in the developing brain. J Neurosci. 1996;16(17):5523-35.

Bitar MS, Pilcher CW, Khan I, Waldbillig RJ. Diabetes-induced suppression of IGF-1 and its receptor mRNA levels in rat superior cervical ganglia. Diabetes Res Clin Pract. 1997;38(2):73-80.

Bithell A, Johnson R, Buckley NJ. Transcriptional dysregulation of coding and non-coding genes in cellular models of Huntington's disease. Biochem Soc Trans. 2009;37(Pt 6):1270-5.

Björkqvist M, Fex M, Renström E, Wierup N, Petersén A, Gil J, Bacos K, Popovic N, Li JY, Sundler F, Brundin P, Mulder H. The R6/2 transgenic mouse model of Huntington's disease develops diabetes due to deficient beta-cell mass and exocytosis. Hum Mol Genet. 2005;14(5):565-74.

Boesgaard TW, Nielsen T, Josefsen K, Hansen T, Jørgensen T, Pedersen O, Nørremølle O, Nielsen JE and Hasholt L. Huntington's Disease Does Not Appear to Increase the Risk of Diabetes Mellitus. Journal of Neuroendocrinology 2009, 21, 770–776.

Bowling AC, Beal MF. Bioenergetic and oxidative stress in neurodegenerative diseases. Life Sci. 1995;56(14):1151-71.

Brinkman RR, Mezei MM, Theilman J, Almqvist E, Hayden MR. The likelihood of being affected with Huntington disease by a particular age, for a specific CAG size. Am J Hum Genet 1997;60:1202-1210

Broderick P, Rahni D, Kolodny H. Bioimaging in Neurodegeneration Totowa, NJ: Humana Press, New Jersey, 2005.

Brüning JC, Winnay J, Bonner-Weir S, Taylor SI, Accili D, Kahn CR.et al. Development of a novel polygenic model of NIDDM in mice heterozygous for IR and IRS-1 null alleles. Cell. 1997; 88:561-572.

Brunet A., Datta, S.R., and Greenberg, M.E. Transcription dependent and -independent control of neuronal survival by the PI3K-Akt signaling pathway. Curr. Opin. Neurobiol. 2001; 11, 297–305.

Carter RJ, Hunt MJ, Morton AJ. Environmental stimulation increases survival in mice transgenic for exon 1 of the Huntington's disease gene. Mov Disord. 2000;15(5):925-37.

Carter RJ, Morton J, Dunnett SB. Motor coordination and balance in rodents. Curr Protoc Neurosci. 2001;Chapter 8.

Carvalho E, Kotani K, Peroni OD, Kahn BB. Adipose-specific overexpression of GLUT4 reverses insulin resistance and diabetes in mice lacking GLUT4 selectively in muscle. Am J Physiol Endocrinol Metab. 2005 Oct;289(4): 551-561.

Caviston JP, Ross JL, Antony SM, Tokito M, Holzbaur EL. Huntingtin facilitates dynein/dynactin-mediated vesicle transport. Proc Natl Acad Sci U S A. 2007, 104(24):10045-50

Chiu SL, Cline HT. Insulin receptor signaling in the development of neuronal structure and function. Neural Dev. 2010, 15;5:7.

Cho KJ, Lee BI, Cheon SY, Kim HW, Kim HJ, Kim GW. Inhibition of apoptosis signal-regulating kinase 1 reduces endoplasmic reticulum stress and nuclear huntingtin fragments in a mouse model of Huntington disease. Neuroscience. 2009; 163(4):1128-34.

Chong SS, Almqvist E, Telenius H, LaTray L, Nichol K, Bourdelat-Parks B, Goldberg YP, Haddad BR, Richards F, Sillence D, Greenberg CR, Ives E, Van den Engh G, Hughes MR, Hayden MR. Contribution of DNA sequence and CAG size to mutation frequencies of intermediate alleles for Huntington disease: evidence from single sperm analyses. Hum Mol Genet. 1997;6(2):301-9.

Chu, C. Autophagic Stress in Neuronal Injury and Disease. J Neuropathol Exp Neurol. 2006 May; 65(5): 423–432.

Cicchetti, F., Parent, A., Striatal interneurons in Huntington's disease: selective increase in the density of calretinin-immunoreactive medium-sized neurons. Mov. Disord. 1996, 11, 619–626.

Conneally P. Huntington Disease: Genetics and Epidemiology. Am J Hum Genet 1984,36:506-526.

Costa MC, Magalhães P, Ferreirinha F, Guimarães F, Januário C, Gaspar I, Loureiro L, Vale J, Garrett C, Regateiro F, Magalhães M, Sousa A, Maciel P, Sequeiros J. Molecular diagnosis of Huntington disease in Portugal: implications for genetic counseling and clinical practice. European Journal of Human Genetics 2003; 11, 872–878

Cuturic M, Abramson RK, Vallini D, Frank EM, Shamsnia M. Sleep patterns in patients with Huntington's disease and their unaffected first-degree relatives: a brief report. Behav Sleep Med. 2009;7(4):245-54.

Damiano M, Galvan L, Déglon N, Brouillet E. Mitochondria in Huntington's disease Biochimica et Biophysica Acta (BBA) - Molecular Basis of Disease. 2010; 1802(1):52-61.

Damiano M, Galvan L, Déglon N, Brouillet E. Mitochondria in Huntington's disease. Biochim Biophys Acta. 2010;1802(1):52-61.

Deng Y. P., Albin R. L., Penney J. B., Young A. B., Anderson K. D., Reiner A. Differential loss of striatal projection systems in Huntington's disease: a quantitative immunohistochemical study. Journal of Chemical Neuroanatomy. 2004; 27:143–164.

Devaskar SU, Giddings SJ, Rajakumar PA, Carnaghi LR, Menon RK, Zahm DS. Insulin gene expression and insulin synthesis in mammalian neuronal cells. J Biol Chem. 1994;269(11):8445-54.

Di Prospero N, Fischbeck K. Therapeutics development for triplet repeat expansion diseases. Nature 2005, 6:756-765

DiFiglia M, Sapp E, Chase KO, Davies SW, Bates GP, Vonsattel JP, Aronin N. Aggregation of huntingtin in neuronal intranuclear inclusions and dystrophic neurites in brain. Science 1997; 277:1990-3.

Djoussé L, Knowlton B, Cupples LA, Marder K, Shoulson I, Myers RH. Weight loss in early stage of Huntington's disease. Neurology. 2002;59(9):1325-30.

Dunah AW, Jeong H, Griffin A, Kim YM, Standaert DG, Hersch SM, Mouradian MM, Young AB, Tanese N, Krainc D. Sp1 and TAFII130 transcriptional activity disrupted in early Huntington's disease. Science 2002; 296(5576):2238-43. Epub 2002 May 2.

Duyao M, Ambrose C, Myers R, Novelletto A, Persichetti F, Frontali M,Folstein S, Ross C, Franz M, Abbott M,.Trinucleotide repeat length instability and age of onset in Huntington's disease. Nature Genetics 1993, 4:387-392.

Fan MM, Raymond LA. N-methyl-D-aspartate (NMDA) receptor function and excitotoxicity in Huntington's disease. Prog Neurobiol. 2007;81(5-6):272-93.

Farrer LA. Diabetes mellitus in Huntington's disease. Clin Genet. 1985;27(1):62-67.

Fecke W, Gianfriddo M, Gaviraghi G, Terstappen GC, Heitz F. Small molecule drug discovery for Huntington's Disease. Drug Discov Today. 2009;14(9-10):453-64.

Ferrante, R.J., Kowall, N.W., Beal, M.F., Martin, J.B., Bird, E.D., Richardson Jr., E.P. Morphological and histochemical characteristics of a spared subset of striatal neurons in Huntington's disease. J. Neuropathol.Exp. Neurol. 1987, 46: 12–27.

Ferrante, R.J., Kowall, N.W., Beal, M.F., Richardson Jr., E.P., Bird, E.D., Martin, J.B. Selective sparing of a class of striatal neurons in Huntington's disease. Science 1985, 230: 561–563.

Ferrante, R.J., Kowall, N.W., Richardson Jr., E.P., Bird, E.D., Martin, J.B., Topography of enkephalin, SP, and acetylcholinesterase staining in Huntington's disease striatum. Neurosci. Lett 1986, 71: 283–288.

Ferrante; R. Mouse models of Huntington's disease and methodological considerations for therapeutic trials. Biochim Biophys Acta. 2009, 1792(6):506-20.

Finkbeiner S, Mitra S. The ubiquitin-proteasome pathway in Huntington's disease. ScientificWorldJournal. 2008; 8:421-33.

Folstein SE, Chase GA, Wahl WE, McDonnell AM, Folstein MF. Huntington's disease in Maryland: clinical aspects of racial variation. Am J Hum Genet 1987; 41:168-179

Foroud T, Gray J, Ivashina J, Conneally P. Differences in duration of Huntington's disease based on age at onset. J Neurol Neurosurg Psychiatry 1999;66:52–56

Frattali, AL, Treadway, JL, Pessin, JE. Insulin/IGF-1 hybrid receptors: implications for the dominant- negative phenotype in syndromes of insulin resistance. J Cell Biochem 1992. 48:43-50.

Furtado S, Suchowersky O, Rewcastle B, Graham L, Klimek ML, Garber A. Relationship between trinucleotide repeats and neuropathological changes in Huntington disease. Ann Neurol 1996;39:132-136.

Fusco FR, Chen Q, Lamoreaux WJ, Figueredo-Cardenas G, Jiao Y, Coffman JA, Surmeier DJ, Honig MG, Carlock LR, Reiner A. Cellular localization of huntingtin in striatal and cortical neurons in rats: lack of correlation with neuronal vulnerability in Huntington's disease. J Neurosci. 1999;19(4):1189-202.

Gaba AM, Zhang K, Marder K, Moskowitz CB, Werner P, Boozer CN. Energy balance in early-stage Huntington disease. Am J Clin Nutr 2005;81:1335–41

Gatchel J, Zoghbi H. Diseases of unstable repeat expansion: mechanisms and common principles. Nature 2005, 6:743-755.

Gauthier, L.R., Charrin, B.C., Borrell-Pages, M., Dompierre, J.P., Rangone, H., Cordelieres, F.P., De Mey, J., MacDonald, M.E., Lessmann, V., Humbert, S. & Saudou, F. Huntingtin controls neurotrophic support and survival of neurons by enhancing BDNF vesicular transport along microtubules. Cell, 2004; 118:127–138.

Goellner, G.M. and Rechsteiner, M. Are Huntington's and polyglutamine based ataxias proteasome storage diseases? Int. J. Biochem. Cell Biol 2003; 35:562–571.

Goldberg YP, Kremer B, Andrew SE, Theilmann J, Graham RK, Squitieri F, Telenius H, Adam S, Sajoo A, Starr E,. Molecular analysis of new mutations for Huntington's disease: intermediate alleles and sex of origin effects. Nat Genet. 1993;5(2):174-9.

Goodman AO, Murgatroyd PR, Medina-Gomez G, Wood NI, Finer N, Vidal-Puig AJ, Morton AJ, Barker RA. The metabolic profile of early Huntington's disease- a combined human and transgenic mouse study. Experimental Neurology 2008; 210: 691–698

Gopalakrishnan L, Scarpulla RC. Differential regulation of respiratory chain subunits by a CREB-dependent signal transduction pathway. Role of cyclic AMP in cytochrome c and COXIV gene expression. J Biol Chem. 1994;269(1):105-13.

Gould T, Dao D, Kovacsics C. The Open Field Test Neuromethods, 2009;42: 1-20

Graham RK, Pouladi MA, Joshi P, Lu G, Deng Y, Wu NP, Figueroa BE, Metzler M, André VM, Slow EJ, Raymond L, Friedlander R, Levine MS, Leavitt BR, Hayden MR. Differential susceptibility to excitotoxic stress in YAC128 mouse models of Huntington disease between initiation and progression of disease. J Neurosci. 2009; 29(7):2193-204.

Graham RK, Pouladi MA, Joshi P, Lu G, Deng Y, Wu NP, Figueroa BE, Metzler M, André VM, Slow EJ, Raymond L, Friedlander R, Levine MS, Leavitt BR, Hayden MR. Differential susceptibility to excitotoxic stress in YAC128 mouse models of Huntington disease between initiation and progression of disease. J Neurosci. 2009 Feb 18;29(7):2193-204.

Gusella et al. A novel gene containing a trinucleotide repeat that is expanded and unstable on Huntington's disease chromosomes. The Huntington's Disease Collaborative Research Group. Cell. 1993;72(6):971-83.

Gusella, J. F. et al. A polymorphic DNA marker genetically linked to Huntington’s disease. Nature 1983,306: 234–238.

Gutekunst CA, Li SH, Yi H, Mulroy JS, Kuemmerle S, Jones R, Rye D, Ferrante RJ, Hersch. SM, Li XJ. Nuclear and neuropil aggregates in Huntington’s disease: Relationship to neuropathology. J Neurosci 1999; 19:2522-34.

Guyton A, Hall J. Fisiologia Humana e Mecanismos das Doenças. 6ª ed. Guanabara Koogan, Rio de Janeiro, 1998.

Haluzik M, Colombo C, Gavrilova O, Chua S, Wolf N, Chen M, Stannard B, Dietz KR, Le Roith D, Reitman ML. Genetic background (C57BL/6J versus FVB/N) strongly influences the severity of diabetes and insulin resistance in ob/ob mice. Endocrinology. 2004;145(7):3258-64.

Hansotia P, Wall R., Berendes. Sleep disturbances and severity of Huntington's disease. Neurology 1985;35:1672

Harper P. The epidemiology of Huntington's disease. Hum Genet 1992, 89: 365-376

Harrington K.M., Kowall N.W., 1991. Parvalbumin immunoreactive neurons resist degeneration in Huntington's disease striatum. J. Neuropathol. Exp. Neurol. 50: 309.

Hoffner G, Djian P. Transglutaminase and diseases of the central nervous system. Frontiers Biosc 2005; 10:3078-92.

Hoffner G, Island ML, Djian P. Purification of neuronal inclusions of patients with Huntington disease reveals a broad range of N-terminal fragments of expanded huntingtin and insoluble polymers. J Neurochem 2005; 95:125-36.

Hoffner G, Souès S, Djian P. Aggregation of expanded huntingtin in the brains of patients with Huntington disease. Prion. 2007;1(1):26-31.

Http://ec.europa.eu/health/ph_information/dissemination/diseases/neuro_en.htm#7 (consulted at 06/oct/2009)

Http://www.healthscout.com/ency/68/275/main.html#cont (consulted at 06/oct/2009)

Hunt MJ, Morton AJ. Atypical diabetes associated with inclusion formation in the R6/2 mouse model of Huntington's disease is not improved by treatment with hypoglycaemic agents. Exp Brain Res. 2005;166(2):220-9.

Huntington G: On chorea. Med Surg Rep 1872; 26:317–321. Republished at: J Neuropsychiatry Clin Neurosci,2003;15: 109 - 112.

James DE, Piper RC. Insulin resistance, diabetes, and the insulin-regulated trafficking of GLUT-4. J Cell Biol. 1994;126(5):1123-6.

Jana NR, Tanaka M, Wang G, Nukina N. Polyglutamine length-dependent interaction of Hsp40 and Hsp70 family chaperones with truncated N-terminal huntingtin: their role in suppression of aggregation and cellular toxicity. Hum Mol Genet. 2000; 9(13):2009-18.

Jones BJ, Roberts DJ. The quantiative measurement of motor inco-ordination in naive mice using an acelerating rotarod. . J Pharm Pharmacol 1968 Apr;20(4):302-4.

Josefsen K, Nielsen MD, Jørgensen KH, Bock T, Nørremølle A, Sørensen SA, Naver B, Hasholt L. Impaired glucose tolerance in the R6/1 transgenic mouse model of Huntington's disease. J Neuroendocrinol. 2008;20(2):165-72.

Kahlem P, Green H, Djian P. Transglutaminase action imitates Huntington's disease: Selective polymerization of huntingtin containing expanded polyglutamine. Mol Cell 1998; 1:595-601.

Kaltenbach LS, Romero E, Becklin RR, Chettier R, Bell R, Phansalkar A, Strand A, Torcassi C, Savage J, Hurlburt A, Cha GH, Ukani L, Chepanoske CL, Zhen Y, Sahasrabudhe S, Olson J,

Kurschner C, Ellerby LM, Peltier JM, Botas J, Hughes RE. Huntingtin interacting proteins are genetic modifiers of neurodegeneration. PLoS Genet. 2007;3(5):e82.

Karpuj MV, Garren H, Slunt H, Price DL, Gusella J, Becher MW, Steinman L. Transglutaminase aggregates huntingtin into nonamyloidogenic polymers, and its enzymatic activity increases in Huntington's disease brain nuclei. Proc Natl Acad Sci U S A. 1999;96(13):7388-93.

Kieburtz K, MacDonald M, Shih C, Feigin A, Steinberg K, Bordwell K, Zimmerman C, Srinidhi J, Sotack J, Gusella J. Trinucleotide repeat length and progression of illness in Huntington's disease. Journal of Medical Genetics 1994;31:872-874.

Koroshetz WJ, Jenkins BG, Rosen BR, Beal MF. Energy metabolism defects in Huntington's disease and effects of coenzyme Qlo. Ann Neurol 1997;41:160-165.

Kremer HP, Roos RA, Dingjan G, Marani E, Bots GT: Atrophy of the hypothalamic lateral tuberal nucleus in Huntington's disease.J Neuropathol Exp Neurol 1990; 49:371-382.

Lalić NM, Marić J, Svetel M, Jotić A, Stefanova E, Lalić K, Dragaševic N, Milicić T, Lukić L, Kostić VS. Glucose homeostasis in Huntington disease: abnormalities in insulin sensitivity and early-phase insulin secretion. Arch Neurol 2008; 65: 476–480.

Landles C, Bates GP. Huntingtin and the molecular pathogenesis of Huntington's disease. Fourth in Molecular Medicine Review Series. EMBO Rep. 2004;5(10):958-63.

Lawrence MC, McKern NM, Ward CW. Insulin receptor structure and its implications for the IGF-1 receptor. Curr Opin Struct Biol. 2007;17(6):699-705.

Li SH, Cheng AL, Zhou H, Lam S, Rao M, Li H, Li XJ. Interaction of Huntington disease protein with transcriptional activator Sp1. Mol Cell Biol.; 22(5):1277-87.

Li SH, Li XJ. Huntingtin-protein interactions and the pathogenesis of Huntington's disease. Trends Genet. 2004;20(3):146-54.

Lumsden A. L., Henshall, T. L., Dayan, S., Lardelli, M. T. and Richards, R. I. Huntingtin-deficient zebrafish exhibit defects in iron utilization and development. Hum. Mol. Genet. 2007; 16, 1905-1920.

Ma Y, Eidelberg D. Functional imaging of cerebral blood flow and glucose metabolism in Parkinson's disease and Huntington's disease. Mol Imaging Biol. 2007 ;9(4):223-33.

Manak M.M. Sample preparation. In DNA probes (ed. G.H. Keller and M.M. Manak) 1993, pp. 27--68. Stockton Press, New York.

Mangiarini L, Sathasivam K, Seller M, Cozens B, Harper A, Hetherington C, Lawton M, Trottier Y, Lehrach H, Davies SW, Bates GP. Exon 1 of the HD gene with an expanded CAG repeat is

sufficient to cause a progressive neurological phenotype in transgenic mice. Cell 1996, 87:493-506.

Marder K, Sandler S, Lechich A, Klager J., Albert S. Relationship between CAG repeat length and late-stage outcomes in Huntington's disease. Neurology 2002;59:1622-1624

Margolis R, Ross C. Diagnosis of Huntington Disease. Clinical Chemistry 2003, 49: 1726-1732; 10.1373/49.10.1726

Martin WR, Wieler M, Hanstock CC. Is brain lactate increased in Huntington's disease? J Neurol Sci. 2007 ;263(1-2):70-4.

Mitra S, Finkbeiner S. The Ubiquitin-Proteasome Pathway in Huntington's Disease. ScientificWorldJournal. ; 8: 421–433.

Modregger J, DiProspero NA, Charles V, Tagle DA, Plomann M. PACSIN 1 interacts with huntingtin and is absent from synaptic varicosities in presymptomatic Huntington's disease brains.Hum Mol Genet. 2002;11(21):2547-58.

Montoya A, Price B, Menear M, Lepage M. Brain imaging and cognitive dysfunctions in Huntington's disease. Rev Psychiatr Neurosci 2006;31(1): 21–29.

Myers RH, MacDonald ME, Koroshetz WJ, Duyao MP, Ambrose CM, Taylor SA, Barnes G, Srinidhi J, Lin CS, Whaley WL. De novo expansion of a (CAG)n repeat in sporadic Huntington's disease. Nat Genet. 1993;5(2):168-73.

Myers RH, Sax DS, Koroshetz WJ, Mastromauro C, Cupples LA, Kiely DK, Pettengill FK, Bird ED. Factors Associated With Slow Progression in Huntington's Disease. Arch Neurol.1991; 48: 800-804.

Nance M, Myers R. Juvenile Onset Huntington's Disease— Clinical and Research Perspectives. Mental Retardation and Developmental Disabilities Research Reviews. 2001,7: 153–157.

Nance MA, Mathias-Hagen V, Breningstall G, Wick MJ, McGlennen RC. Analysis of a very large trinucleotide repeat in a patient with juvenile Huntington's disease. Neurology. 1999;52(2):392-4.

Naver B, Stub C, Møller M, Fenger K, Hansen AK, Hasholt L, Sørensen SA. Molecular and behavioral analysis of the R6/1 Huntington's disease transgenic mouse, Neuroscience 122 2003;1049–1057.

Neylan T. Neurodegenerative Disorders: George Huntington's Description of Hereditary Chorea. J Neuropsychiatry Clin Neurosci. 2003;15: 108.

Nordström CH. Insulin, intracerebral glucose and bedside biochemical monitoring utilizing microdialysis. Crit Care. 2008;12(2):124.

Nørremølle A, Rless O, Eppien J, Fenger K, Hasholt L, Sørensen S. Trinucleotide repeat elongation in the Huntingtin gene in Huntington Disease patients from 71 Danish families. Hum. Mol. Genet..1993; 2: 1475-1476

Nucifora FC Jr, Sasaki M, Peters MF, Huang H, Cooper JK, Yamada M, Takahashi H, Tsuji S, Troncoso J, Dawson VL, Dawson TM, Ross CA. Interference by huntingtin and atrophin-1 with cbp-mediated transcription leading to cellular toxicity. Science. 2001; 291(5512):2423-8.

Oliveira JM, Jekabsons MB, Chen S, Lin A, Rego AC, Gonçalves J, Ellerby LM, Nicholls DG. Mitochondrial dysfunction in Huntington's disease: the bioenergetics of isolated and in situ mitochondria from transgenic mice. J Neurochem. 2007;101(1):241-9.

Owen OE, Morgan AP, Kemp HG, Sullivan JM, Herrera MG, Cahill GF Jr. Brain metabolism during fasting. J Clin Invest. 1967;46(10):1589-95.

Pellerin L, Magistretti PJ Glutamate uptake into astrocytes stimulates aerobic glycolysis: a mechanism coupling neuronal activity to glucose utilization. 1994, Proc Natl Acad Sci USA 91, 10625–10629.

Perutz MF, Johnson T, Suzuki M, Finch JT. Glutamine repeats as polar zippers: Their possible role in inherited neurodegenerative diseases. Proc Natl Acad Sci 1994; 91:5355- 8.

Petersén A, Gil J, Maat-Schieman ML, Björkqvist M, Tanila H, Araújo IM, Smith R, Popovic N, Wierup N, Norlén P, Li JY, Roos RA, Sundler F, Mulder H, Brundin P. Orexin loss in Huntington's disease. Hum Mol Genet. 2005;14(1):39-47.

Podolsky S, Leopold NA. Abnormal glucose tolerance and arginine tolerance tests in Huntington's disease. Gerontology. 1977;23(1):55-63.

Potter N, Spector E, Prior T. American College Of Medical Genetics. Standards and Guidelines for Clinical Genetics Laboratories. Technical Standards and Guidelines for Huntington Disease. Genet Med 2004;6(1):61–65.

Pouladi MA, Xie Y, Skotte NH, Ehrnhoefer DE, Graham RK, Kim JE, Bissada N, Yang XW, Paganetti P, Friedlander RM, Leavitt BR, Hayden MR. Full-length huntingtin levels modulate body weight by influencing insulin-like growth factor 1 expression. Hum Mol Genet. 2010;19(8):1528-38.

Pradet A, Raymond P. Adenine Nucleotide Ratios and Adenylate Energy Charge in Energy Metabolism. Annual Review of Plant Physiology, 1983; 34: 199-224.

Pratley RE, Salbe AD, Ravussin E, Caviness JN. Higher sedentary energy expenditure in patients with Huntington's disease. Annals of neurology. 2000,47(1):64-70

Purves D, Augustine G, Fitzpatric D, Hall W, Lamantia AS, McNamara J, Williams S. Neuroscience Chapter 17, 3 ed. Massachusetts U.S.A. 2004.

Quarrell OWJ, Tyler A, Jones MP, Nordin M, Harper PS. Population studies of Huntington's disease in Wales. Clin Genet 1988; 33:189-195

Quintanillaa R, Johnson G. Role of mitochondrial dysfunction in the pathogenesis of Huntington's disease. Brain Research Bulletin 2009; 80: 242–247.

Rego A, Almeida L. Molecular Targets and Therapeutic Strategies in Huntington's Disease. Current Drug Targets - CNS & Neurological Disorders, 2005, 4: 361-381

Reiner A, Albin RL, Anderson KD, D'Amato CJ, Penney JB, Young AB. Differential loss of striatal projection neurons in Huntington disease. Proc Natl Acad Sci U S A. 1988;85(15):5733-7.

Rosenblatt A, Liang RY, Zhou H, Abbott MH, Gourley LM, Margolis R L, Brandt J, Ross CA. The association of CAG repeat length with clinical progression in Huntington disease. Neurology 2006;66:1016-1020

Ross C. Margolis R. Huntington's disease Clinical Neuroscience Research. 2001;142:152

Rubinsztein DC, Leggo J, Coles R, Almqvist E, Biancalana V, Cassiman JJ, Chotai K, Connarty M, Crauford D, Curtis A, Curtis D, Davidson MJ, Differ AM, Dode C, Dodge A, Frontali M, Ranen NG, Stine OC, Sherr M, Abbott MH, Franz ML, Graham CA, Harper PS, Hedreen JC, Hayden MR. Phenotypic characterization of individuals with 30-40 CAG repeats in the Huntington disease (HD) gene reveals HD cases with 36 repeats and apparently normal elderly individuals with 36-39 repeats. Am J Hum Genet. 1996;59(1):16-22.

Rubinsztein DC. Lessons from animal models of Huntington's disease. Trends Genet. 2002 Apr;18(4):202-9.

Ruocco HH, Lopes-Cendes I, Laurito TL, Li LM, Cendes F. Clinical presentation of juvenile Huntington disease. Arq Neuropsiquiatr. 2006;64(1):5-9.

Sadri-Vakili G, Cha JH. Mechanisms of disease: Histone modifications in Huntington's disease. Nat Clin Pract Neurol. 2006;2 (6):330-8.

Sapp E, Schwarz C, Chase K. Huntingtin localization in brains of normal and Huntington's disease patients. Ann Neurol 1997;42:604–12.

Sattler UG, Walenta S, Mueller-Klieser W. A bioluminescence technique for quantitative and structure-associated imaging of pyruvate. Lab Invest. 2007;87(1):84-92.

Sawa A, Wiegand GW, Cooper J, Margolis RL, Sharp AH, Lawler JF Jr, Greenamyre JT, Snyder SH, Ross CA. Increased apoptosis of Huntington disease lymphoblasts associated with repeat length-dependent mitochondrial depolarization. Nat Med. 1999;5(10):1194-8.

Schauwecker P. Modulation of Cell Death by Mouse Genotype: Differential Vulnerability to Excitatory Amino Acid-Induced Lesions Experimental Neurology, 2002, 178(2): 219-235

Schauwecker, P.E., Steward, O. Genetic determinants of susceptibility to excitotoxic cell death: implications for gene targeting approaches. Proc. Natl. Acad. Sci .U. S. A 1997; 94, 4103–4108.

Schilling G, Becher MW, Sharp AH, Jinnah HA, Duan K, Kotzuk JA, Slunt HH, Ratovitski T, Cooper JK, Jenkins NA, Copeland NG, Price DL, Ross CA, Borchelt DR. Intranuclear inclusions and neuritic aggregates in transgenic mice expressing a m N-terminal fragment of huntingtin. Hum Mol Genet. 1999;8(3):397-407.

Sedewitz B, Schleifer KH, Götz F. Purification and biochemical characterization of pyruvate oxidase from Lactobacillus plantarum. J Bacteriol. 1984 Oct;160(1):273-8.

Seneca S, Fagnart D, Keymolen K, Lissens W, Hasaerts D, Debulpaep S, Desprechins B, Liebaers I, De Meirleir L. Early onset Huntington disease: a neuronal degeneration syndrome. Eur J Pediatr. 2004;163(12):717-21.

Shehadeh J, Fernandes HB, Zeron Mullins MM, Graham RK, Leavitt BR, Hayden MR, Raymond LA. Striatal neuronal apoptosis is preferentially enhanced by NMDA receptor activation in YAC transgenic mouse model of Huntington disease. Neurobiol Dis. 2006; 21(2):392-403.

Sieradzan K, Mann DM, Dodge A. Clinical presentation and patterns of regional cerebral atrophy related to the length of trinucleotide repeat expansion in patients with adult onset Huntington's disease. Neurosci Lett. 1997; 225(1):45-8.

Singaraja RR, Hadano S, Metzler M, Givan S, Wellington CL, Warby S, Yanai A, Gutekunst CA, Leavitt BR, Yi H, Fichter K, Gan L, McCutcheon K, Chopra V, Michel J, Hersch SM, Ikeda JE, Hayden MR. HIP14, a novel ankyrin domain-containing protein, links huntingtin to intracellular trafficking and endocytosis. Hum Mol Genet. 2002; 11(23):2815-28.

Sittler A, Wälter S, Wedemeyer N, Hasenbank R, Scherzinger E, Eickhoff H, Bates GP, Lehrach H, Wanker EE. SH3GL3 associates with the Huntingtin exon 1 protein and promotes the formation of polygln-containing protein aggregates. Mol Cell. 1998; 2(4):427-36.

Smith R, Brundin P, Li JY. Synaptic dysfunction in Huntington's disease: a new perspective. Cell Mol Life Sci. 2005;62(17):1901-12.

Smith R, Petersén A, Bates GP, Brundin P, Li JY. Depletion of rabphilin 3A in a transgenic mouse model (R6/1) of Huntington's disease, a possible culprit in synaptic dysfunction. Neurobiol Dis. 2005; 20(3):673-84.

Sørensen SA, Fenger K. Causes of death in patients with Huntington's disease and in unaffected first degree relatives. J Med Genet 1992; 29: 91 1-914

Stack EC, Kubilus JK, Smith K, Cormier K, Del Signore SJ, Guelin E, Ryu H, Hersch SM, Ferrante RJ. Chronology of behavioral symptoms and neuropathological sequela in R6/2 Huntington's disease transgenic mice. J Comp Neurol. 2005, 490(4):354-70.

Starling AJ, André VM, Cepeda C, de Lima M, Chandler SH, Levine MS. Alterations in N-methyl-D-aspartate receptor sensitivity and magnesium blockade occur early in development in the R6/2 mouse model of Huntington's disease. J Neurosci Res. 2005;82(3):377-86.

Steffan JS, Kazantsev A, Spasic-Boskovic O, Greenwald M, Zhu YZ, Gohler H, Wanker EE, Bates GP, Housman DE, Thompson LM. The Huntington's disease protein interacts with p53 and CREB-binding protein and represses transcription. Proc Natl Acad Sci U S A. 2000; 97(12):6763-8.

Stocchi V, Cucchiarini L, Magnani M, Chiarantini L, Palma P, Crescentini G Simultaneous extraction and reverse-phase high-performance liquid chromatographic determination of adenine and pyridine nucleotides in human red blood cells. Anal. Biochem. 1985; 146: 118–124

Taketo M, Schroeder AC, Mobraaten LE, Gunning KB, Hanten G, Fox RR, Roderick TH, Stewart CL, Lilly F, Hansen CT. FVB/N: an inbred mouse strain preferable for transgenic analyses. Proc Natl Acad Sci U S A. 1991;88(6):2065-9.

Tang TS, Slow E, Lupu V, Stavrovskaya IG, Sugimori M, Llinás R, Kristal BS, Hayden MR, Bezprozvanny I. Disturbed Ca2+ signaling and apoptosis of medium spiny neurons in Huntington's disease. Proc Natl Acad Sci U S A. 2005;102(7):2602-7.

Timmers H.J., Swaab, D.F., van de Nes, J.A. & Kremer, H.P. Somatostatin 1–12 immunoreactivity is decreased in the hypothalamic lateral tuberal nucleus of Huntington's disease patients. Brain Res. 1996, 728:141–148.

Trejo A, Tarrats RM, Alonso ME, Boll MC, Ochoa A, Velásquez L.. Assessment of the nutrition status of patients with Huntington's disease. Nutrition. 2004;20(2):192-6.

Trejo JL, Carro E, Garcia-Galloway E, Torres-Aleman I. Role of insulin-like growth factor I signaling in neurodegenerative diseases. J Mol Med. 2004;82(3):156-62.

Trottier Y, Devys D, Imbert G, Saudou F, An I, Luta Y, Weber C, Agid Y, Hirsch EC, Mandel J-L Cellular localization of the Huntington's disease protein and discrimination of the normal and mutated form. Nature Genet. 1995; 10:104 –110.

Trushina E, Singh RD, Dyer RB, Cao S, Shah VH, Parton RG, Pagano RE, McMurray CT. Mutant huntingtin inhibits clathrin-independent endocytosis and causes accumulation of cholesterol in vitro and in vivo. Hum Mol Genet. 2006;15(24):3578-91.

van Duijn E, Kingma EM, van der Mast RC. "Psychopathology in verified Huntington's disease gene carriers". J Neuropsychiatry Clin Neurosci. 2007;19(4):441–8.

Van Raamsdonk JM, Metzler M, Slow E, Pearson J, Schwab C, Carroll J, Graham RK, Leavitt BR, Hayden MR. Phenotypic abnormalities in the YAC128 mouse model of Huntington disease are penetrant on multiple genetic backgrounds and modulated by strain. Neurobiol Dis. 2007;26(1):189-200.

Van Raamsdonk JM, Warby SC, Hayden MR. Selective degeneration in YAC mouse models of Huntington disease. Brain Res Bull. 2007; 72(2-3):124-31.

Vonsattel, J.P., Myers, R.H., Stevens, T.J., Ferrante, R.J., Bird, E.D. & Richardson, E.P., Jr. Neuropathological classification of Huntington's disease. J. Neuropathol. Exp. Neurol., 1985;44: 559–577.

Vonsattel, J.-P.G., DiFiglia, M., Huntington disease. J. Neuropathol. Exp. Neurol. 1998;57: 369–384

Walker F. Huntington's disease. Lancet 2007; 369: 218–28.

Wang J, Wang CE, Orr A, Tydlacka S, Li SH, Li XJ. Impaired ubiquitin-proteasome system activity in the synapses of Huntington's disease mice. J Cell Biol. 2008; 180(6):1177-89.

Wellington C, Ellerby L, Leavittc B, Roy S, Nicholson D, Hayden M. Huntingtin proteolysis in Huntington disease. Clinical Neuroscience Research 2003;3 (3):129-139.

Wellington C.L., Ellerby L.M., Gutekunst C.A., Rogers D., Warby S., Graham R.K., Loubser O., van Raamsdonk J., Singaraja R., Yang Y.Z.. Caspase cleavage of m huntingtin precedes neurodegeneration in Huntington's disease. J. Neurosci. 2002; 22, 7862–7872.

Wellington CL, Ellerby LM, Hackam AS, Margolis RL, Trifiro MA, Singaraja R, McCutcheon K, Salvesen GS, Propp SS, Bromm M, Rowland KJ, Zhang T, Rasper D, Roy S, Thornberry N, Pinsky L, Kakizuka A, Ross CA, Nicholson DW, Bredesen DE, Hayden MR Caspase

cleavage of gene products associated with triplet expansion disorders generates truncated fragments containing the polyglutamine tract. J Biol Chem 1998, 273:9158-9167.

Wellington CL, Singaraja R, Ellerby L, Savill J, Roy S, Leavitt B, Cattaneo E, Hackam A, Sharp A, Thornberry N, Nicholson DW, Bredesen DE, Hayden MR Inhibiting caspase cleavage of huntingtin reduces toxicity and aggregate formation in neuronal and nonneuronal cells. J Biol Chem 2000, 275:19831-19838

Weydt P, Pineda VV, Torrence AE, Libby RT, Satterfield TF, Lazarowski ER, Gilbert ML, Morton GJ, Bammler TK, Strand AD, Cui L, Beyer RP, Easley CN, Smith AC, Krainc D, Luquet S, Sweet IR, Schwartz MW, La Spada AR. Thermoregulatory and metabolic defects in Huntington's disease transgenic mice implicate PGC-1alpha in Huntington's disease neurodegeneration. Cell Metab. 2006;4(5):349-62.

Wiegand M., Miiller A, Clauer CJ, Stolz S, Schreiber W, Dose M,Krieg JC. Nocturnal sleep in Huntington's disease. J Neurol. 1991; 238:203-208

Wild E J, Tabrizi S J. The differential diagnosis of chorea. Pract Neurol 2007; 7: 360–373.

Wong FS, Janeway CA Jr. Insulin-dependent diabetes mellitus and it animal models (review). Current Opinion in Immunology 1999,11(6): 643-7.

Wright HM, Still CN, Ramson RK. Huntington's disease in black kindreds in South Carolina. Arch Neurol 1981, 38:412-414

Wu J, Lin F, Qin Z. Sequestration of glyceraldehyde-3-phosphate dehydrogenase to aggregates formed by m huntingtin. Acta Biochim Biophys Sin. 2007;39(11):885-90.

Yamanaka T, Miyazaki H, Oyama F, Kurosawa M, Washizu C, Doi H, Nukina N. M Huntingtin reduces HSP70 expression through the sequestration of NF-Y transcription factor. EMBO J. 2008;27(6):827-39.

Yang SH, Cheng PH, Banta H, Piotrowska-Nitsche K, Yang JJ, Cheng EC, Snyder B, Larkin K, Liu J, Orkin J, Fang ZH, Smith Y, Bachevalier J, Zola SM, Li SH, Li XJ, Chan AW. Towards a transgenic model of Huntington's disease in a non-human primate. Nature. 2008, 453(7197):921-4.

Yoo E; Lee S. Glucose Biosensors: An Overview of Use in Clinical Practice. Sensors 2010, 10, 4558-4576

Zhang H, Li Q, Graham RK, Slow E, Hayden MR, Bezprozvanny I. Full length m huntingtin is required for altered Ca2+ signaling and apoptosis of striatal neurons in the YAC mouse model of Huntington's disease. Neurobiol Dis. 2008; 31(1):80-8.

Zhang S, Feany MB, Saraswati S, Littleton JT, Perrimon N. Inactivation of Drosophila Huntingtin affects long-term adult functioning and the pathogenesis of a Huntington's disease model. Dis Model Mech. 2009; 2(5-6):247-66.

Zou, K. H. Comparisons of correlated receiver operating characteristic curves derived from repeated diagnostic test data. Acad. Radiol. 2001; 8, 225-233.

Zuccato C, Tartari M, Crotti A, Goffredo D, Valenza M, Conti L, Cataudella T, Leavitt BR, Hayden MR, Timmusk T, Rigamonti D, Cattaneo E. Huntingtin interacts with REST/NRSF to modulate the transcription of NRSE-controlled neuronal genes. Nat Genet. 2003;35(1):76-83.